



## Performance Evaluation and Cost Analysis of Photovoltaic Thermal (PVT) System Using the Triangular Shape of Absorber with Different Water-based Nanofluids as Coolants

Mrigendra Singh<sup>1\*</sup>, S.C Solanki<sup>1</sup>, Basant Agrawal<sup>2</sup> and Rajesh Bhargava<sup>3</sup>



<sup>1</sup>Mechanical Engineering Department, Ujjain Engineering College, Ujjain, M.P.-456010, India;

<sup>2</sup>Mechanical Engineering Department, Shri G. S. Institute of Technology and Science, Indore, M.P.-452003,

India; <sup>3</sup>Rajiv Gandhi Proudyogiki Vishwavidyalaya, Bhopal, M.P.-462033, India

### E-mail/Orcid Id:

MS, [mrigendra.rits@gmail.com](mailto:mrigendra.rits@gmail.com), <https://orcid.org/0009-0006-2737-4127>; SC, [subhashsolanki95@yahoo.co.in](mailto:subhashsolanki95@yahoo.co.in), <https://orcid.org/0009-0000-7196-944X>; BA, [bas\\_agr@yahoo.co.in](mailto:bas_agr@yahoo.co.in), <https://orcid.org/0000-0002-7798-6272>; RB, [dy.registrarrgv@gmail.com](mailto:dy.registrarrgv@gmail.com), <https://orcid.org/0009-0005-5008-9626>

### Article History:

Received: 09<sup>th</sup> Dec., 2023

Accepted: 16<sup>th</sup> May, 2024

Published: 30<sup>th</sup> May, 2024

### Keywords:

Cost analysis, Electrical and thermal efficiency, Nanofluids, PVT system, Pressure drop, Solar energy

### How to cite this Article:

Mrigendra Singh, S.C Solanki, Basant Agrawal and Rajesh Bhargava (2024). Performance Evaluation and Cost Analysis of Photovoltaic Thermal (PVT) System Using the Triangular Shape of Absorber with Different Water-based Nanofluids as Coolants. *International Journal of Experimental Research and Review*, 39(spl.) 51-72.

DOI: <https://doi.org/10.52756/ijerr.2024.v39spl.004>

**Abstract:** The worldwide energy demand is continuously increasing, prompting experts to recommend using alternative energy sources to conserve natural gas, fossil fuels, and electricity. Photovoltaic thermal (PVT) systems emerge as a viable solution, generating electrical and heat energy simultaneously while freeing carbon dioxide (CO<sub>2</sub>) emissions. These systems offer sustainable green technology for supplying renewable electricity and heat to commercial and domestic applications. This study delves into the performance of a photovoltaic thermal (PVT) system featuring an isosceles triangular-shaped absorber design. It considers size variations of 0.02 and 0.03 m while maintaining a constant aspect ratio. Water-based nanofluids such as CuO/w, MgO/w, and ZnO/w, with a nanoparticle volume portion of 4%, alongside pure water as a coolant, are utilized with a variation of mass flow rate ranges from 0.028 kg/s to 0.11 kg/s, allowing for an exploration of its impact on performance parameters. A numerical model is established to comprehensively analyze the system's performance, applying an energy balance equation to its components. An economic analysis is also conducted to assess the system's cost-effectiveness and determine the energy payback time. Results indicate that the highest overall daily performance is achieved with ZnO/w nanofluid at a mass flow rate of 0.112 kg/s and a fluid flow channel size of 0.02 m. Comparatively, compared to other nanofluids and pure water, the average electrical, thermal, and overall performances achieved are 14.57%, 22.36%, and 36.40%, respectively. The energy payback periods are 5.5, 5.2, 5.4, and 4.8 years for CuO/w, MgO/w, ZnO/w, and Pure water, respectively. Furthermore, it is observed that a higher mass flow rate correlates with higher system performance parameters.

### Introduction

There is a growing demand for energy to ensure human comfort in the present era. However, the predominant reliance on fossil fuels for energy generation poses significant environmental challenges due to greenhouse gas emissions contributing to climate change. Renewable energy emerges as a crucial solution to mitigate these concerns. Solar energy is an abundant and environmentally friendly option among renewable sources. Solar energy, available universally, can be

harnessed effectively using technologies such as heat collectors and PV panels to convert it into valuable energy resources (Hegedus and Luque, 2003). It converts only 10-16% of the penetrated sun radiation into electrical energy; the rest of the radiation is reflected in the atmosphere in heat (Al-Waeli et al., 2018). It is known that an overheated PV panel reduces the performance.

PV panel temperature increases of 1°C may affect 0.5% and 0.25% performance reductions for crystalline



and amorphous silicon PV panels (Lee et al., 2019). Therefore, removing the buildup heat from the rear surface of the PV panel is required to maintain a working temperature. The removed heat energy can be utilized for crop drying, space heating, and water heating. For this purpose, a PVT collector hybrid technique could produce electrical and heat energy simultaneously. It is a combination of PV and solar thermal systems (Azad et al., 2024; Hissouf et al., 2020b). The heat of the PV panel is extracted by cooling fluids like air and liquids circulating in fluid flow channels underneath the PV panel. The cooling fluid absorbs the excessive heat and maintains a relatively lower temperature for the PV panel (Gao et al., 2019). As a result, the cooling channels' thermal performance affects the system's overall efficiency (Nasrin et al., 2018). Numerous design considerations influence the performance of PVT systems, including factors like mass transfer rate, number of glass covers, the thermal conductivity of coolant, and design of the absorber channel (shape, diameter and thickness) (Charalambous et al., 2007). Researchers have conducted diverse studies to enhance the performance of PVT systems by using different coolant and absorber channel designs. In the initial stages, work focused on air and water cooling systems. Different research has been carried out on the different designs of the PVT system with air as the cooling fluid, such as single and double-pass PVT air collectors and V-down ribs (Deo et al., 2016; Kamthania et al., 2011; Tiwari et al., 2006).

Concurrently, different researchers used water as a cooling fluid in PVT systems and concluded that the effectiveness of PVT water collectors is superior to air (Buonomano et al., 2019; Herrando et al., 2014). PVT water thermal system helps achieve the electrical energy and hot water demand for different places. However, the performance of the PVT system is improved using the traditional fluid air and water; the prospect of improvement needs to be improved because the traditional fluids used for heat extraction carry a lower heat transfer rate. The thermal properties of traditional fluids may be enhanced by nanoparticles such as metals, oxides, carbides, or carbon nanotubes in base fluid, called nanofluids. Nanofluids are formulated by dispersing solid particles of nanometric dimensions into a primary solvent (Sani et al., 2010). Hence, the heat removal rate of the nanofluids is higher than that of the primary solvent. The nanofluids' thermo physical property depends on the volume concentration, sonication time and size of nanoparticles (Madhesh and Kalaiselvam, 2015). Consequently, there has been different research on the impact of nanofluids, volume concentration, and fluid

flow methods with variations in the mass flow rate of the PVT systems (Javadi et al., 2013).

Sardarabadi et al. (2014) examined the impact of SiO<sub>2</sub>/w nanofluid at 3% volume portion and pure water in sheet- and tube-type PVT collectors and obtained the total exergy improved by 7.9% compared to PVT water collector. Al-Shamani et al. (2016) experimentally examined the performance of PVT collectors using nanofluids (SiO<sub>2</sub>, TiO<sub>2</sub> and SiC) with rectangular tube fluid flow channels and obtained the SiC nanofluid giving higher performance of 81.73% and 13.25% in terms of thermal and electrical efficiency as compared to other nanofluids. Zhou et al. (2018) optimize the cooling channels' design to examine the temperature variation of a PVT system equipped with a serpentine tube. The study focuses on how the temperature variation is impacted by the design of the winding cooling tube. It is helpful to carefully evaluate both the channels' low pressure and thermal impact.

Kazem et al. (2020) carried out experimental and numerical analysis of the PVT system using web, direct, and spiral flow arrangements, and it is fixed that spiral flow tubes generate a higher performance of 35% compared to other flow arrangements. Hissouf et al. (2020b) Investigate the performance of a PVT collector employing two cooling fluids in circular, semi-circular, and square-shaped fluid flow channel configurations and find out that the semi-circle channel design has the maximum performance and best photovoltaic cooling effect compared to other geometries, increasing thermal efficiency by 1.17% and 2.5% compared to other channels. Similarly (Yu et al., 2021) investigated the performance of the PVT system with periodically grooved channels and found that the average temperature of the PVMs with PEGs is about 4 K lower than that with smooth channels. It also finds out the pressure drop of the flow channel and maximum pressure drop achieved by rectangular column grooves compared with semi-cylinder and triangular column-shaped grooves.

Kong et al. (2022) optimize the design of the PVT collector with internal corrugated channels and observe the influencing parameters such as the corrugation number, area, and the flow channel width on the exit temperature of the hybrid PVT system and found that the width of the absorber plate is reduced the exit temperature is increased. Khan et al. (2022) conducted an experimental study to examine the effectiveness of a PVT system with a serpentine tube employing Fe<sub>3</sub>O<sub>4</sub>/w, SiO<sub>2</sub>/w, and Fe<sub>3</sub>O<sub>4</sub>/SiO<sub>2</sub> nanofluids at volume portions of 3% wt at varied flow rates of 20, 30, and 40 LPM and achieved the most significant electricity efficiency is

12.6%, 18.46%, and 24.3%, respectively at 40 LPM. Madas et al. (2023) carried out a TRNSYS-based numerical evaluation to investigate the performance of the PVT systems using nano-copper oxide (CuO) at volume portions between 0.10 % and 0.50 % and mass transfer at 60, 80, and 120 kg/h. using. And obtained that at 60 kg/h transfer rate, enhancement in the electrical and thermal performance by 1.11 and 3.30 % similarly (Azad et al., 2024) numerical investigation is carried out to determine the performance parameters using the CNT nanofluids as a coolant addition, regression analyses are carried out for determining the effect of variable of electrical and thermal efficiency.

On the other hand, the cost of the PVT system plays a vital role in domestic and commercial uses. Consequently, numerous academics have investigated the economic and exergoeconomic analysis of the PVT system and evaluated its cost-effectiveness of the PVT system. Agrawal and Tiwari (2015) annualized the performance of glazed PVT air collectors in terms of carbon credit and cost and concluded that carbon emission reduction comes to Rs 109,242 and Rs 25275.6 based on overall thermal energy and exergy basis. Somasundaram and Tay (2019) investigate the performance and economic analysis of the PVT system. Findings are represented in terms of internal rate of return, net present value, and payback duration. Jidhesh et al. (2021) conducted a numerical and experimental study to investigate the performance of a semitransparent PVT collector using CuO nanofluid and water as a coolant and analyze the cost of the system in terms of payback duration. Bin Ishak et al. (2023) investigate the performance and economic analysis of a PVT collector using reversed circular flow jet impingement with a variation of mass flow rate ranging from 0.01 to 0.014 kg/s and found that maximum electrical performance is 11.38% at sun radiation 500 w/m<sup>2</sup> and thermal performance 61.4% under 900 w/m<sup>2</sup> at mass flow rate 0.014 kg/s overall, higher sun radiation is required for energy analysis, and from an economic point of view, less sun irradiance is more suitable.

Based on the available literature, the performance of the PVT system varies with nanofluid and fluid flow methods, as evidenced by past research. The utilization of nanofluids and fluid flow methods is of utmost importance. Nanofluid flow methods are extensively employed on the back side of the PV panel. Past research shows that utilising nanofluid as a coolant and fluid flow method is a captivating area of study. The outcome of the PVT system is enhanced by employing nanofluid and fluid flow methods on the back side of the PV panel. It

was found that more research needs to be conducted on a triangular tube-type fluid flow channel and the effect of the hydraulic diameter on the system's performance. The current system's effectiveness is compared to the previous numerical and experimental work shown in Table 1.

The current study numerically evaluates the performance of PVT systems (sheet and triangular channel) using different nanofluids such as CuO/w, MgO/w, ZnO/w at a volume portion of nanoparticle is 4% with pure water along with water for isosceles triangular shape geometry of fluid flow channel with variation of size 0.02 m to 0.03 m. and addition economic analysis was performed to evaluate the energy payback duration of the system. The primary contribution of current work comprises

- Establishing the numerical formulation for the different layers of the PVT system and validating it against previous results available in the literature determine by the numerical and experimental evaluation.
- Evaluate the electrical and thermal efficiency of the PVT system with variations in mass flow rate 0.028 kg/s, 0.056 kg/s and 0.011kg/s and triangular tube size 0.02 m and 0.03m
- Cost analysis is carried out to evaluate the system's energy payback period.

**Table 1. Performance evaluation of different PVT systems.**

Evaluation type	Nanoparticle volume portion	$\eta_{th}$ (%)	$\eta_{ele}$ (%)	Researcher
Numerical	Al <sub>2</sub> O <sub>3</sub> /w and Cu/w (2%)	35 to 50	12 to 14	Hissouf et al., 2020a
Numerical/experimental	Fe <sub>3</sub> O <sub>4</sub> /w SiO <sub>2</sub> /w (3%)	38 & 40	12.5 and 13.15	Khan et al., 2022
Numerical	Cu/w and Al <sub>2</sub> O <sub>3</sub> /w (2%)	40 to 48	14.2 to 15	Diwania et al., 2021
Numerical/experimental	CuO/w and Al <sub>2</sub> O <sub>3</sub> /w (2%)	38.1 & 35.9	13 and 12.49	Mahmood Alsalame et al., 2021
Numerical	CuO/w, MgO/w, ZnO/w (4%)	21 to 22.27	13.73 to 14.70	<b>Present (Average per day)</b>

## Methodology

### Collector layout & concept

Figure 1 displays the schematic view of a triangular channel-type photovoltaic thermal collector, with a configuration protected by a glass cover and air gap. It consists of a PV cell, a heat-absorbing sheet attached to

the rear side of the PV cell through an adhesive layering of ethylene vinyl acetate (EVA), and a fluid flowing inside the channel fastened to the rear side of the absorber sheet. The energy is transferred through heat transfer liquid flow in a channel. Insulating material covering the collector's corners reduces the heat that escapes through the surface's bottom (Gundala et al., 2021).

plate temperature. Fig.2. explains the flow of heat between different elements. The ensuing presumption is considered for numerical modeling(Gupta et al., 2022; Jidhesh et al., 2021).

1. The heat transfer is presumed to be single-dimensional.
2. The thermo physical properties of nanofluids are

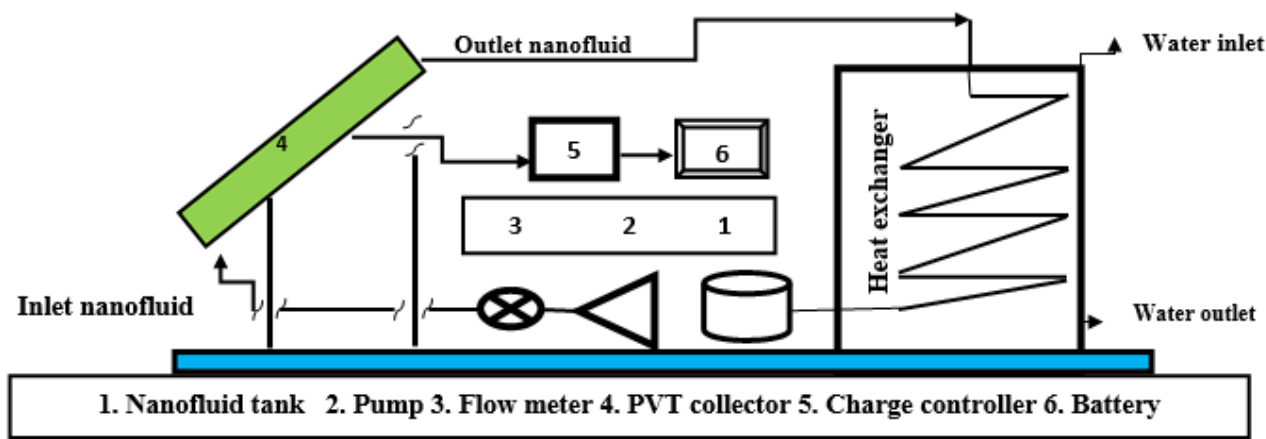


Figure 2. Schematic diagram of the PVT collector

Table 2. Technical specification of the photovoltaic panel (cdvine)

Specifi- cation	Solar module	$P_{max}$	$V_{oc}$ (V)	$I_{sc}$ (A)	$V_{max}$ (V)	$I_{max}$ (A)	$\eta_s$	Working temperature range	Cell type	Cell packing factor
Value	250 W	250W	37.72	8.76	30.3	8.25	15.3%	- 40°C to 85°C	Mono crystalline	0.8

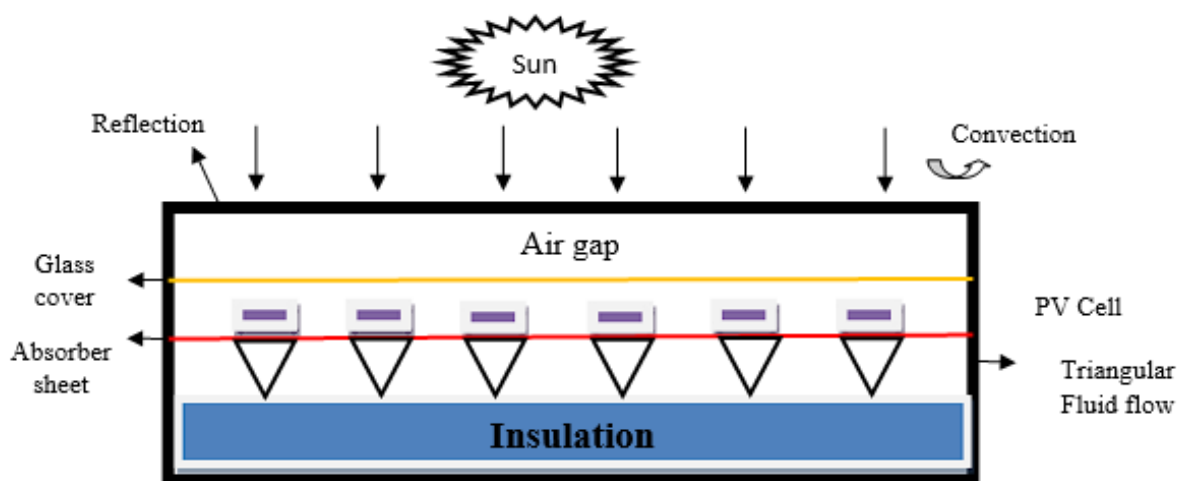


Figure 1. Cross-section view of triangular tube flow channel on PVT collector.

### Heat balance equation for PVT System

Electricity is generated when sunlight penetrates the PV panel through the PVT system, and excess heat is transmitted to the adhesive layer and absorber plate; this heat is absorbed by the coolant liquid flowing through the channel and reducing the adhesive layer and absorber

independent of the temperature.

3. Each component of the PVT system needs to be perfectly insulated.
4. The optical properties of the material remain constant.



## Energy balance equation for PV panel

[Heat consumed by PV panel + heat consumed by nonpacking area] = [Heat loss from the top surface to atmosphere] + [heat transfer between cell to absorber sheet] + [Power generation]

$$\tau_g[\alpha_c\beta_c + \alpha_T(1 - \beta_c)]Gwdx$$

$$= [U_{tc-a}(T_c - T_a) + U_T(T_c - T_{bs})wdx + \tau_g\eta\alpha_c\beta_cGwdx \dots \dots \dots (1)$$

Using equation (1), find the solar cell temperature

$$T_c = \frac{h_t T_{bs} + U_T T_a + (\alpha\tau)eff.G}{U_T + U_{tc-a}} \dots \dots \dots (2)$$

## Energy balance for absorbing sheet

[Heat transfer to the rear side of the absorber sheet] = [Heat transfer to the coolant through the absorber sheet]

$$U_T(T_c - T_{bs})wdx$$

$$= h_{Tf}(T_{bs} - T_f)wdx \dots \dots \dots (3)$$

With help, equation (2) & (3) determine the PV panel's backside temperature expression.

$$T_{bs} = \frac{h_{p1}\tau_g[\alpha_c\beta_c + \alpha_T(1 - \beta_c) - \alpha_c\eta\beta_c]G + U_{tT}T_a + h_{Tf}T_f}{U_{tT} + h_T} \dots (4)$$

## Energy balance for flowing fluid inside the channel

[Heat transferred to the fluid through absorber sheet] = [(Heat contained by the flowing liquid) + (Heat loss from liquid to surrounding through insulation)]

$$h_{Tf}\dot{F}(T_{bs} - T_f)wdx$$

$$= \dot{m}_{nf}C_{nf} \frac{dT_f}{dx} dx + U_{Lgt}(T_f - T_a) \dots \dots \dots (5)$$

Using equation (5), solve the linear differential equation boundary condition  $x=0, T_f = T_{fi}$  &  $x=L, T_f = T_{fo}$  and get the exit temperature of the fluid.

$$T_{fo} = \left\{ \frac{[h_{p1}h_{p2}(\alpha\tau)effG]}{U_{Lgt}} + T_a \right\} \left( 1 - \exp\left(\frac{-A\dot{F}U_{Lgt}}{\dot{m}_{nf}C_{nf}}\right) + T_{fi}\exp\left(\frac{-A\dot{F}U_{Lgt}}{\dot{m}_{nf}C_{nf}}\right) \dots \dots (6)$$

## Effective parameters of the PVT system

### Thermal efficiency:

$$\eta_{th} = \frac{\dot{m}_{nf}C_{pnf}(T_{fo} - T_{fi})}{GA} \dots \dots \dots (7)$$

### Heat gain:

$$Q_{th} = \dot{m}_{nf}C_{pnf}(T_{fo} - T_{fi}) \dots \dots \dots (8)$$

### Temperature-dependent Electrical efficiency

$$\eta_{el} = \eta_{ref}[1 - \beta(T_{pv} - T_{ref})] \dots \dots \dots (9)$$

### The overall efficiency of PVT collector

$$\eta_{ov} = \eta_{elc} + \eta_{th} \dots \dots \dots (10)$$

### Pumping power & pressure drop

The pumping power and pressure drop of the PVT system are calculated by (Jidhesh et al., 2021)

$$E_p = \frac{\dot{m}_{nf}\Delta P}{\rho_{nf}\eta_p} \dots \dots \dots (11)$$

$$\Delta P = \frac{4fl\rho_{nf}V^2}{2d} + \frac{k_{los}\rho_{nf}V^2}{2}$$

$$\text{Where } V = \frac{\dot{m}}{\rho_{nf}A_t} \dots \dots \dots (12)$$

### Heat transfer coefficients for different components

The coefficient of radiated heat transfer between the atmosphere and a photovoltaic panel is assessed by the (Rejeb et al., 2015)

$$h_{rad Pv-a} = \sigma\epsilon_g A (T_g^2 + T_{sky}^2)(T_g + T_{sky}) \dots \dots (13)$$

$$T_{sky} = 0.0552 * T_a^{3/2} \dots \dots \dots (14)$$

The convective heat transfer coefficient and Nusselt number of fluid flowing inside the channel are calculated by (Sardarabadi & Passandideh-Fard, 2016)

$$R_e < 2300, N_u = 4.364 \dots \dots \dots (15)$$

$$R_e > 2300, N_u = 0.023 R_e^{4/5} P_r^{2/5} \dots \dots \dots (16)$$

Where  $P_r$ , and  $R_e$  denote the Prandtl number and Reynolds number of nanofluids.

$$Pr_{nf} = \frac{\mu_{nf} \cdot Cp_{nf}}{K_{nf}}$$

$$\&Re_{nf} = \frac{\rho_{nf} \cdot V \cdot d}{\mu_{nf}} \dots \dots \dots (17)$$

**Thermo physical properties of nanofluids**

The heat capacity and mass density of the nanofluids evaluated by (Pak and Cho, 1998)

$$\rho_{nf} = \phi \cdot \rho_{np} + (1 - \phi)\rho_{bf} \dots \dots \dots (18)$$

$$C_{p,nf} = \frac{\phi (\rho \cdot C_p)_{np} + (1 - \phi)(\rho \cdot C_p)_{bf}}{\rho_{nf}} \dots \dots \dots (19)$$

Dynamic viscosity of nanofluid is calculated by (Brinkman, 1952)

$$\phi < 0.05, \mu_{nf} = (1 + 2.5\phi)\mu_{bf} \dots \dots \dots (20)$$

The rate of heat conductivity of the nanofluids is evaluated by Hamilton and Crosser (1962).

$$K_{nf} = \frac{K_p - 2\phi (K_{bf} - K_p) + 2K_{bf}}{K_p - \phi (K_{bf} - K_p) + 2K_{bf}} \dots \dots \dots (21)$$

**Economical analysis**

The annual electricity generated in India is 1624.15 BU in 2022-23. When 56.8% is a fossil fuel, 12.4% ishydropower, and 30.2% is renewable energy like solar, wind, and others (power). Solar energy is beneficial for

**Table 3. Thermal characteristics of nanoparticles (Deshmukh and Karmare, 2021)(calculated by equations no. 18, 19 and 20).**

Property	Volume Fraction (%)	Density (kg/m <sup>3</sup> )	Heat capacity (J/kgK)	Rate of heat transfer (W/mK)	
Base fluid water	-	998.2	4179	0.61	Default
CuO/w	4%	1201.76	3390.37	1.112615	Calculated
ZnO/w	4%	1166.96	3468.67	1.116769	Calculated
MgO/w	4%	1084.96	3744.04	1.119584	Calculated

reducing GHG emissions and achieving the electricity generation target. The yearly electric energy created by the PVT collector is evaluated.

$$E_{ele} = \eta_{ele} G A_c N_s \dots \dots \dots (22)$$

Yearly thermal energy created by the PVT system is evaluated by:

$$E_{th} = \eta_{th} G A_c N_s \dots \dots \dots (23)$$

Where *G* is yearly sun radiation, and *N<sub>s</sub>* are no. sunshine days every year. The collector's total energy is a combination of electrical current and heat energy produced

by the PVT system. For cost analysis of the PVT collector, different cost factors are considered (Agrawal & Tiwari, 2015): Cost of the PVT system (TCS), yearly maintenance cost (YMC), yearly salvage value (YSV), Yearly running cost of the pump (YRC). The total cost (TC) of the PVT system is the summation of collector cost, maintenance cost, salvage value and running cost of the system is evaluated by:

$$TC = TCS + YRC + YMC - YSV \dots \dots \dots (24)$$

Total collector cost is given by:

$$TCS = CI \times CRF$$

Where CRF is the capital recovery factor is evaluated by  $CRF = i(i + 1)^n \times [(i + 1)^n - 1]^{-1}$

Yearly maintenance cost is accepted as 10% of TCS

YSV is evaluated by  $YSV = SV \times SFF$  where SV is accepted as 10% of CI.

Salvage factor evaluated by:

$$SFF = i \times [(i + 1)^n - 1]^{-1}$$

The yearly saving of the PVT collector due to electric current and heat energy is evaluated by:

$$A P_n = CS_n - TC_n \dots \dots \dots (25)$$

The payback duration can be evaluated by the following equation (Hussain and Kim, 2018):

$$EPBD = \frac{E_{inpute}}{E_{Total}}$$

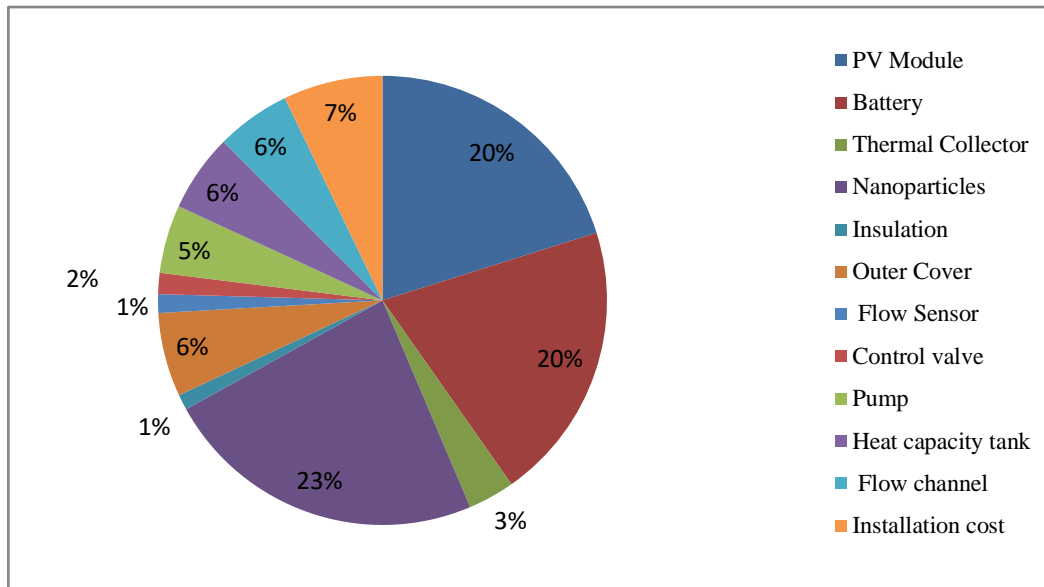


**Figure 3. Distribution of capital cost of nanofluids-based PVT collector.**

**Table 4. Design consideration of the PVT system.**

Components	Parameters	Value	Unit
Glass Cover	Thickness, heat conductivity	0.005, 0.8	m, W/mk
	Transmissivity, Absorptivity	0.95, 0.04	
PV panel	Heat conductivity	100	W/mk
	Absorptance	0.9	
	Module efficiency & Temp. coefficient	15.3%, 0.0045	1/K
Absorber	Thickness, Rate of heat transfer	$6 \times 10^{-4}$ , 380	m, W/mk
Tube	Size of the fluid flow channel	0.02 & 0.03	m
	Total Length and tube spacing	3, 0.1	m
Insulation layer	Thickness, heat conductivity	0.06, 0.028	m, W/mk
Coolant fluid	The inlet temperature of the coolant	299	K
Atmospheric parameters	Average velocity of air, slope angle	1.6, 33°	m/s

### Numerical Procedure

For evaluating the performance of a nanofluid-based PVT collector, the specifications of the PV panel and design parameters of the PVT collector are detailed in Tables (2) and (4), respectively. Subsequently, the numerical formulation is solved using MATLAB program version R-2020 for various components of the system employing different nanofluids (CuO/w, ZnO/w, MgO/w) with a nanoparticle volume portion of 4%, as well as pure water with a variation of the mass flow rate 0.028 kg/s to 0.112 kg/s and size of the absorber channel are varied is 0.02 and 0.03 m while maintaining a constant aspect ratio. Meteorological data, including solar radiation, ambient temperature and airflow velocity in the

atmosphere, were initialized for March 2021 in the Indian city of Ujjain (23.1765° N, 75.7885° E). An average air velocity of 1.6 m/s and an inclination angle of 33° for the collector are considered to calculate the heat transfer between different components. (Hissouf et al., 2020a; Tiwari and Sodha, 2006) The following steps are undertaken.

- Initialize various PVT collector components' geometric, thermal, and optical characteristics.
- Consider the sun radiation, wind velocity, the ambient temperature, and the nanofluid's initial temperature.
- Evaluate the numerical equation and get the performance parameters of the PVT system.
- Evaluate the cost analysis and determine the energy payback period for the PVT system.

## Results and observations

The effectiveness of PVT collectors employing nanofluids is assessed in this work at a volume portion of 4% by weight and pure water as a coolant for triangular tubes for flowing the fluid at different flow velocities and mass flow rates. The hourly variation of sun rays and atmospheric temperature is shown in Figure 4; the sun radiation and atmospheric temperature increase from morning to 12:00 am and decrease from noon to 16:00 pm. The peak value of sun radiation and atmospheric temperature achieved at 12:00 am. is  $823.52 \text{ W/m}^2$  and  $35.63^\circ\text{C}$ , respectively (Resources).

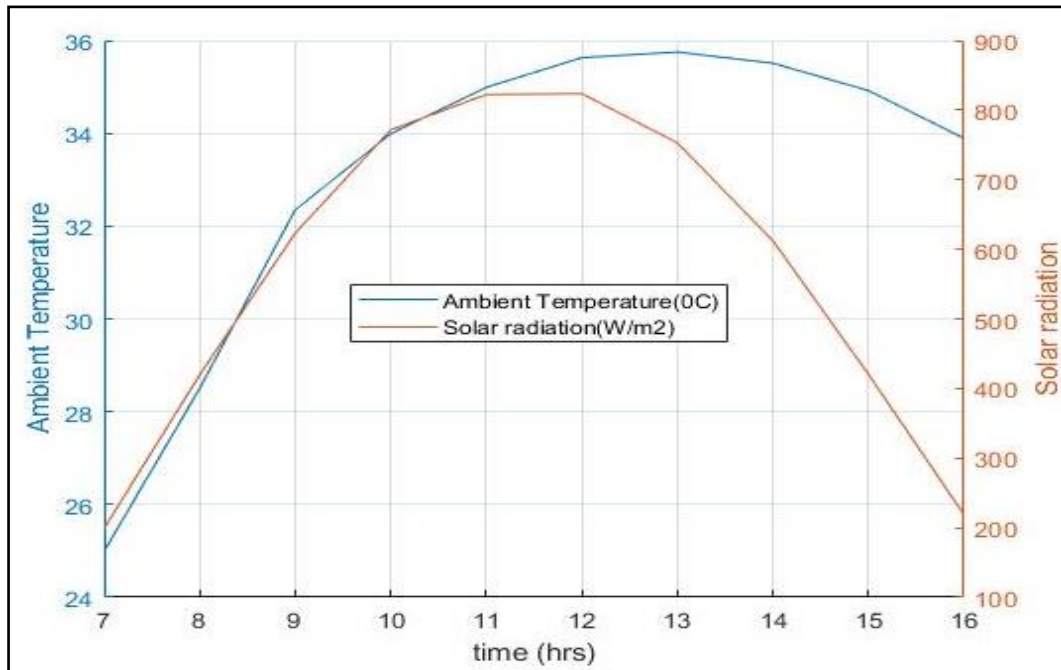
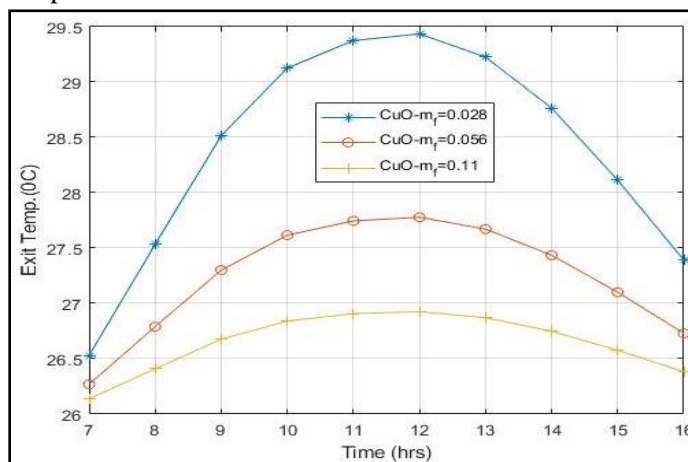


Figure 4. Hourly fluctuation of sun radiation and atmospheric temperature.

### PVT collector exit temperature of nanofluids

Since the PVT collector's exit temperature depends on both solar radiation and ambient temperature, rising solar radiation and ambient temperature raise the nanofluids' exit temperature (Gelis et al., 2023). In this study, the exit temperature of the PVT collector is calculated for

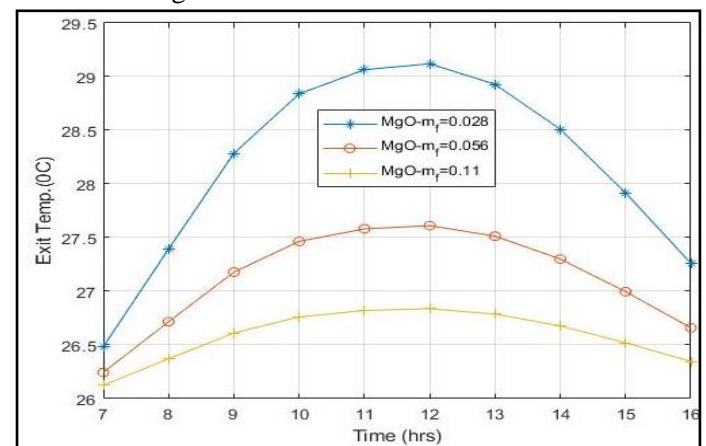


(a)

different nanofluids CuO/w, ZnO/w, MgO/w at the volume portion of nanoparticle is 4% and pure water for isosceles triangular fluid flow channel with a variation of nanofluids flow velocity between  $0.0005 \text{ m/s}$  to  $0.0007 \text{ m/s}$  and the mass flow rate is  $0.028 \text{ kg/s}$  to  $0.112 \text{ kg/s}$ . The size of the isosceles triangular flow channel is  $0.02$  and  $0.03 \text{ m}$ . Figure 5(a-d) displays the hourly variation of exiting temperature with a  $0.02 \text{ m}$  isosceles triangular fluid flow channel size.

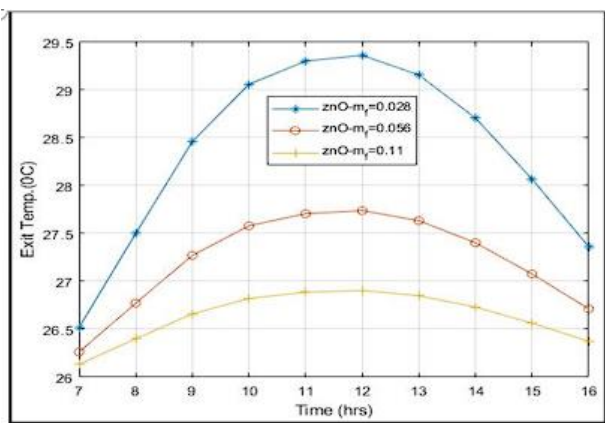
The exit temperature increases from morning to 12:00 a.m. and then decreases from 12:00 a.m. to 16:00 p.m. maximum temperature rises are achieved at 12:00 a.m. It

is observed that exit temperature decreases with increased flow velocity because flow velocity is related to the mass flow rate. The maximum temperature achieved is  $29.43^\circ\text{C}$ ,  $29.36^\circ\text{C}$ ,  $29.11^\circ\text{C}$ , and  $28.71^\circ\text{C}$ , respectively, for CuO/w, ZnO/w, MgO/w, and pure water at mass flow rates  $0.028 \text{ kg/s}$  and sun radiation  $823.52 \text{ W/m}^2$ . On the

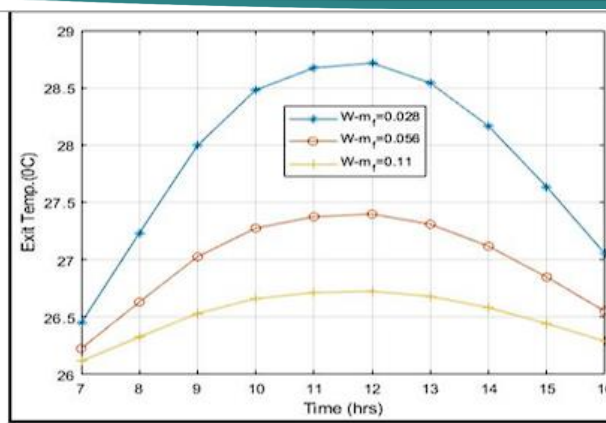


(b)





(c)

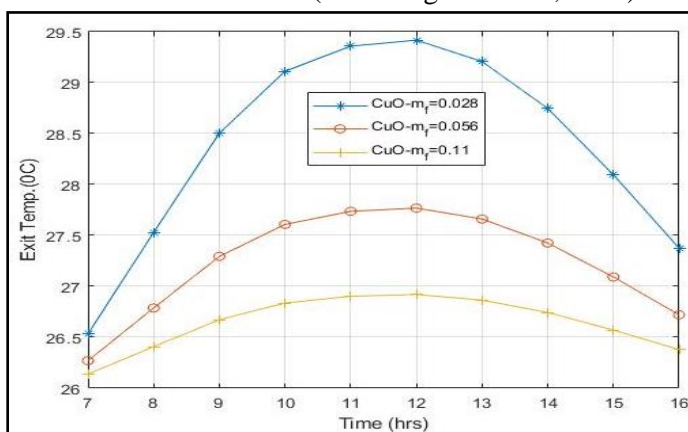


(d)

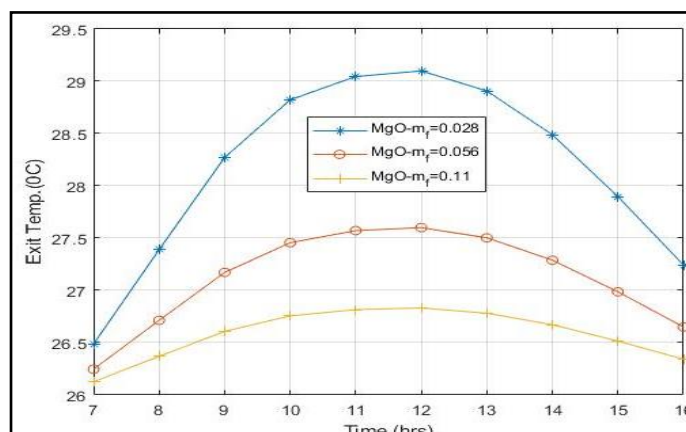
**Figure 5. Hourly fluctuation of exiting temperature (a) CuO/w (b) MgO/w (c) ZnO/w nanofluids (d) Water of PVT system for absorber size 0.02 m.**

other hand, when the fluid flow channel size is increased to 0.03 m, the exit temperature is decreased, as shown in Figure 6 (a-d). Because the size of the fluid flow channel increased, the hydraulic diameter of the channel increased, and due to the increase in the hydraulic diameter of the channel, the heat transfer rate decreased. A minor hydraulic diameter is more suitable for the uniform heat transfer rate (Gunnasegaran et al., 2010).

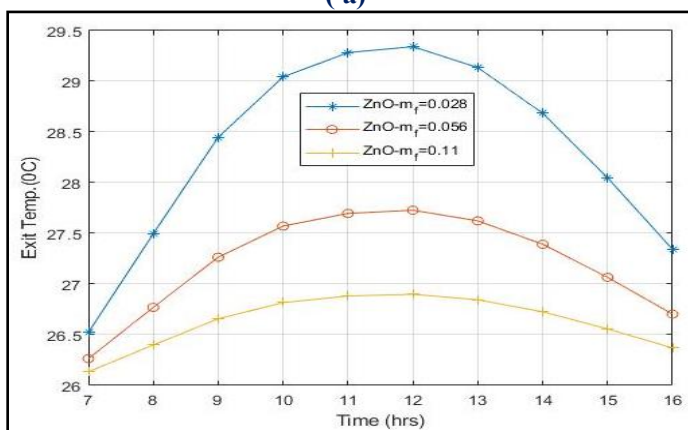
Under this condition, the maximum temperatures for CuO/w, ZnO/w, MgO/w, and Pure water at the same mass flow rate and sun radiation were 29.400C, 29.320C, 29.070C, and 28.640C, respectively. It is clearly shown that nanofluids are more effective than pure water because the higher thermal conductivity of nanofluids removes more heat from the PV panel than water under the same conditions.



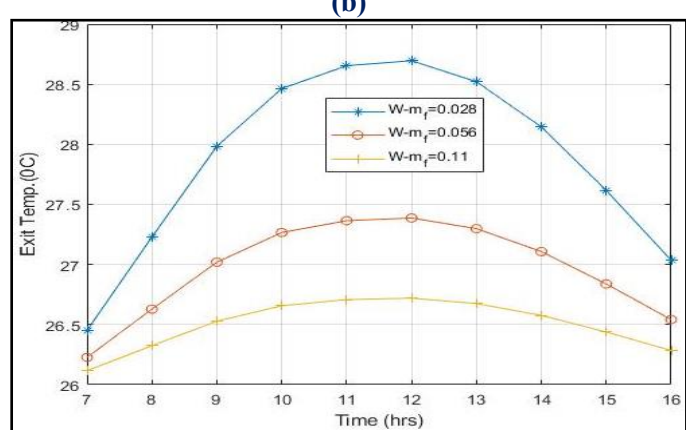
(a)



(b)



(c)



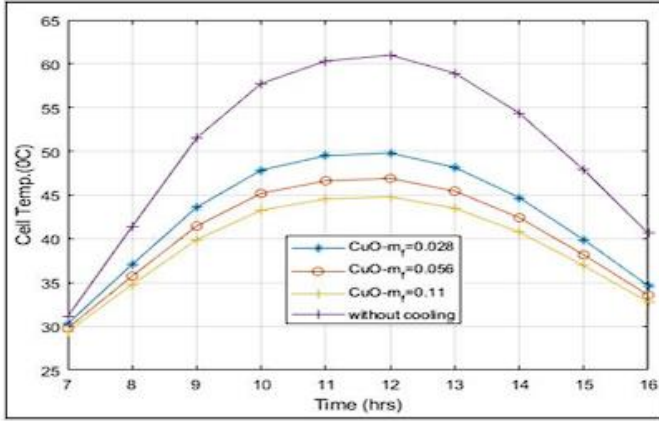
(d)

**Figure 6. Hourly fluctuation of exiting temperature (a) CuO/w (b) MgO/w (c) ZnO/w nanofluids (d) Water of PVT system for absorber size 0.03 m.**

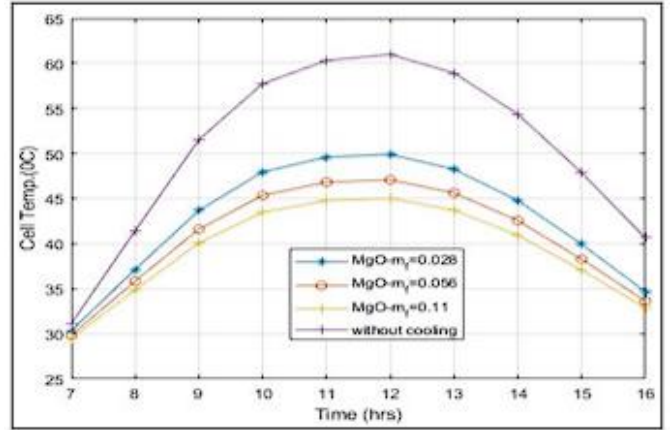
### Cell temperature of PVT collector

Cell temperature of the PV and PVT collector is evaluated for different nanofluids at the volume portion of the nanoparticle is 4% and Pure water for isosceles triangular fluid flow channel with a variation of size 0.02 m and 0.03 m for flow velocity variation between 0.0005 m/s to 0.0007 m/s and the mass flow rate is 0.028 kg/s to 0.112 kg/s.

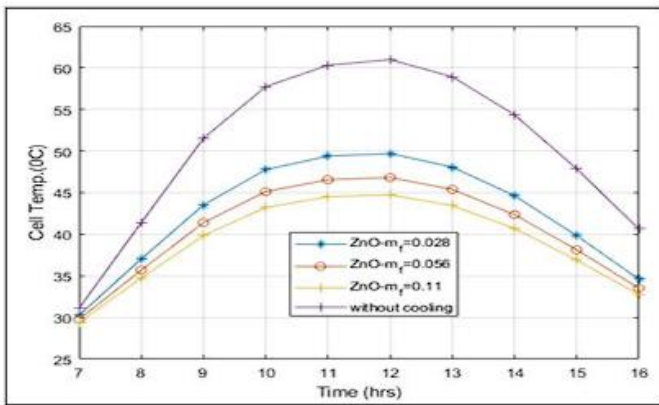
Figure 7(a-d) shows the hourly fluctuation of the cell temperature with a size 0.02 m isosceles triangular fluid flow channel. Cell temperature increases from morning to 12:00 a.m., reaches the maximum temperature and then decreases from 12:00 a.m. to 16:00. It is observed that cell temperature decreases when the mass flow rate increases (Hissouf et al., 2020a). The minimum cell temperature achieved for PVT collector for different ano



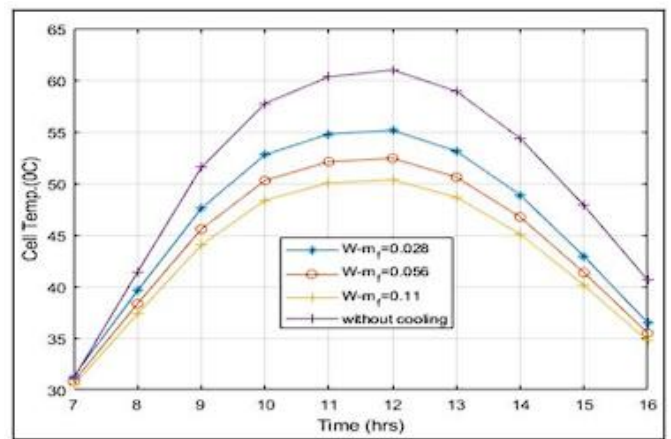
(a)



(b)

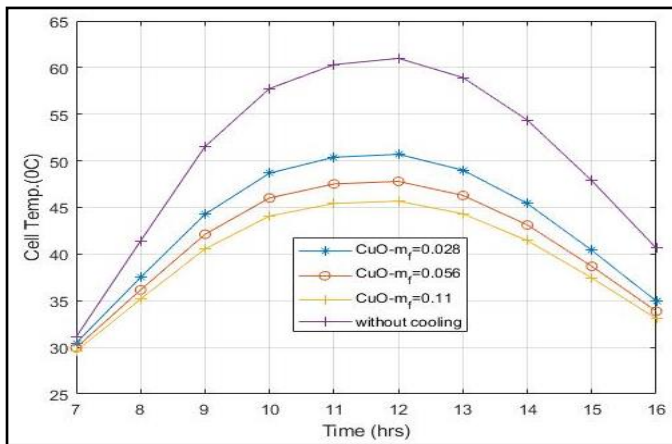


(c)

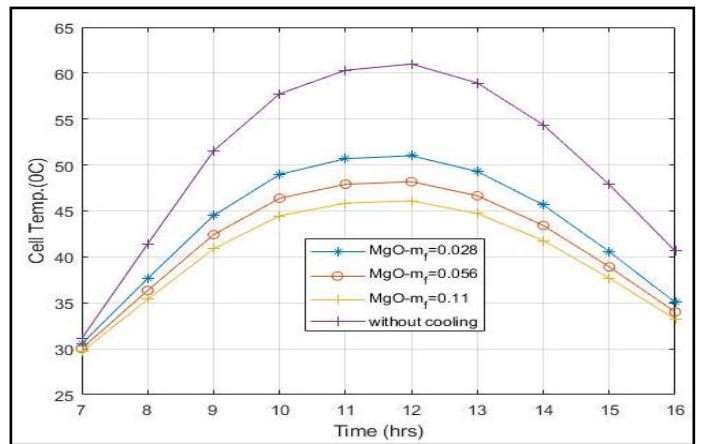


(d)

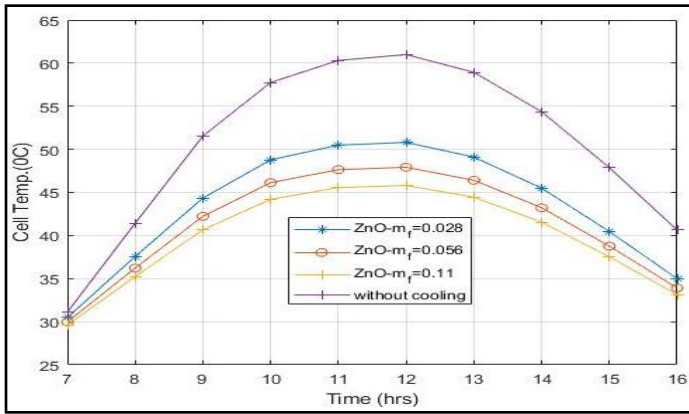
**Figure 7. Hourly fluctuation of cell temperature (a) CuO/w (b) MgO/w (c) ZnO/w nanofluid (d) water of PVT system for absorber size 0.02 m.**



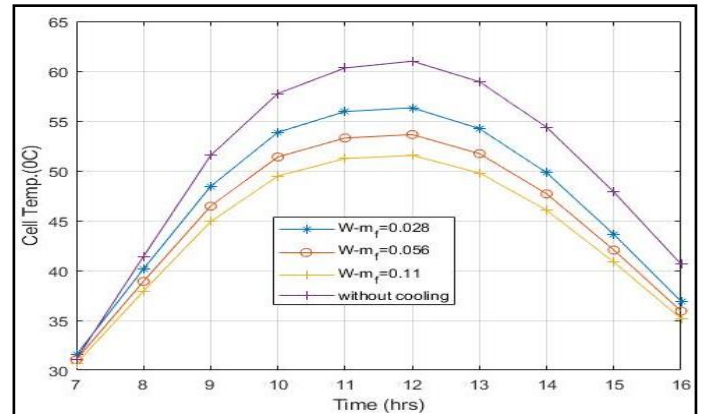
(a)



(b)



(c)

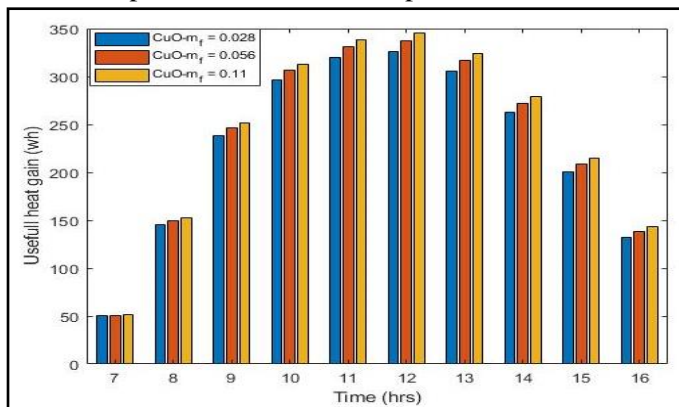


(d)

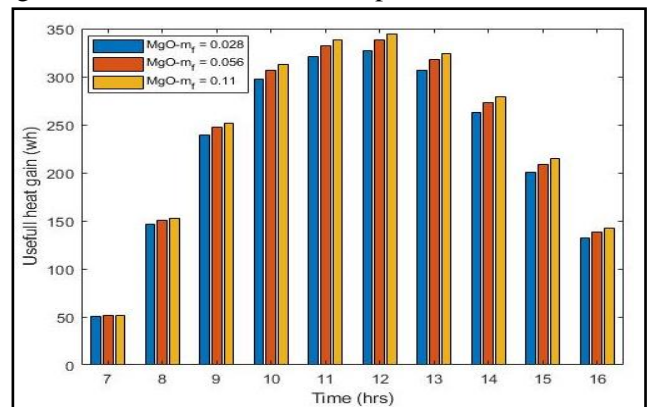
**Figure 8. Hourly fluctuation of cell temperature (a) CuO/w (b) MgO/w (c) ZnO/w nanofluid (d) water of PVT system for absorber size 0.03 m.**

fluids MgO/w, CuO/w, ZnO/w, and pure water is 45.01°C, 44.79°C, 44.73 °C, and 50.34°C at mass flow rate 0.11 kg/s and sun radiation 823.52 W/m<sup>2</sup>, And the maximum temperature achieved for PV without cooling is 60.99 °C at the same condition. It clearly shows that cooling reduces the cell temperature and is helpful to enhance the performance of the PV panel.

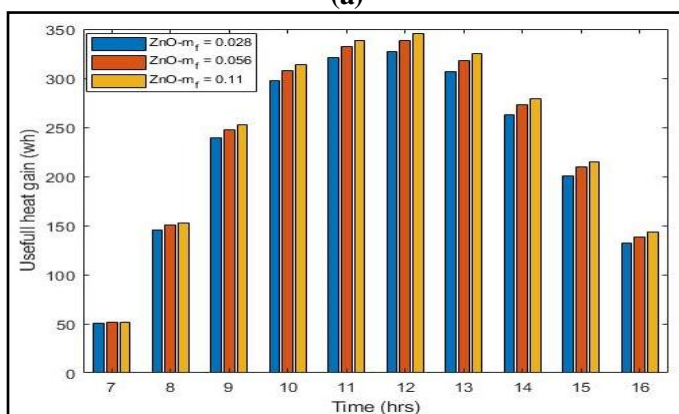
The reason behind that is that the hydraulic diameter of the channel is increased and the rate of heat transfer decreased. For a high heat transfer rate, a minor hydraulic diameter is more suitable (Gunnasegaran et al., 2010). In that case, the minimum temperature achieved was 46.10°C, 45.67°C, 45.80°C, and 51.54°C, respectively, for MgO/w, CuO/w, ZnO/w, and pure water at the same



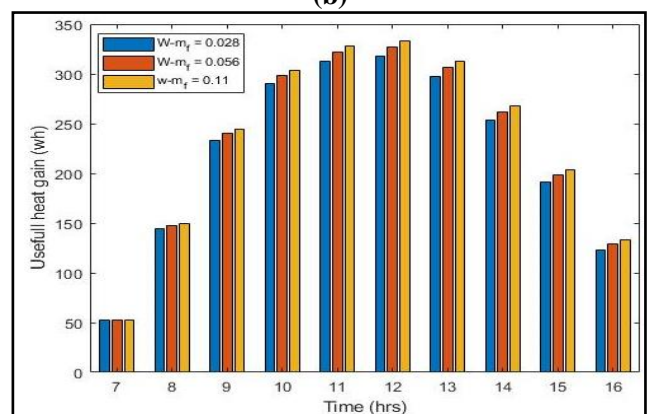
(a)



(b)



(c)



(d)

**Figure 9. Hourly fluctuation of heat gain(a) CuO/w (b) MgO/w (c) ZnO/w nanofluid (d) water of PVT system for absorber size 0.02 m.**

On the other hand, the size of the fluid flow channel is increased to 0.03 m due to the increased cell temperature of the PVT collector, which is displayed in Figure 8(a-d).

condition. This compression shows that a minor hydraulic diameter is more effective for enhancing the performance of the PVT collector.



## Heat gain of PVT system

Heat gain of the system is a function of the specific heat, mass flow rate, and exit temperature of the coolant (Jia et al., 2020). Heat gain is evaluated for the PVT collector using different nanofluids at a volume portion of the nanoparticle of 4% and pure water for isosceles triangular tube fluid flow channels with a flow velocity from 0.0005 m/s to 0.0007 m/s and mass flow rate from 0.028 to 0.11 kg/s. Variation of the size of the fluid flow channel are 0.02 and 0.03 m.

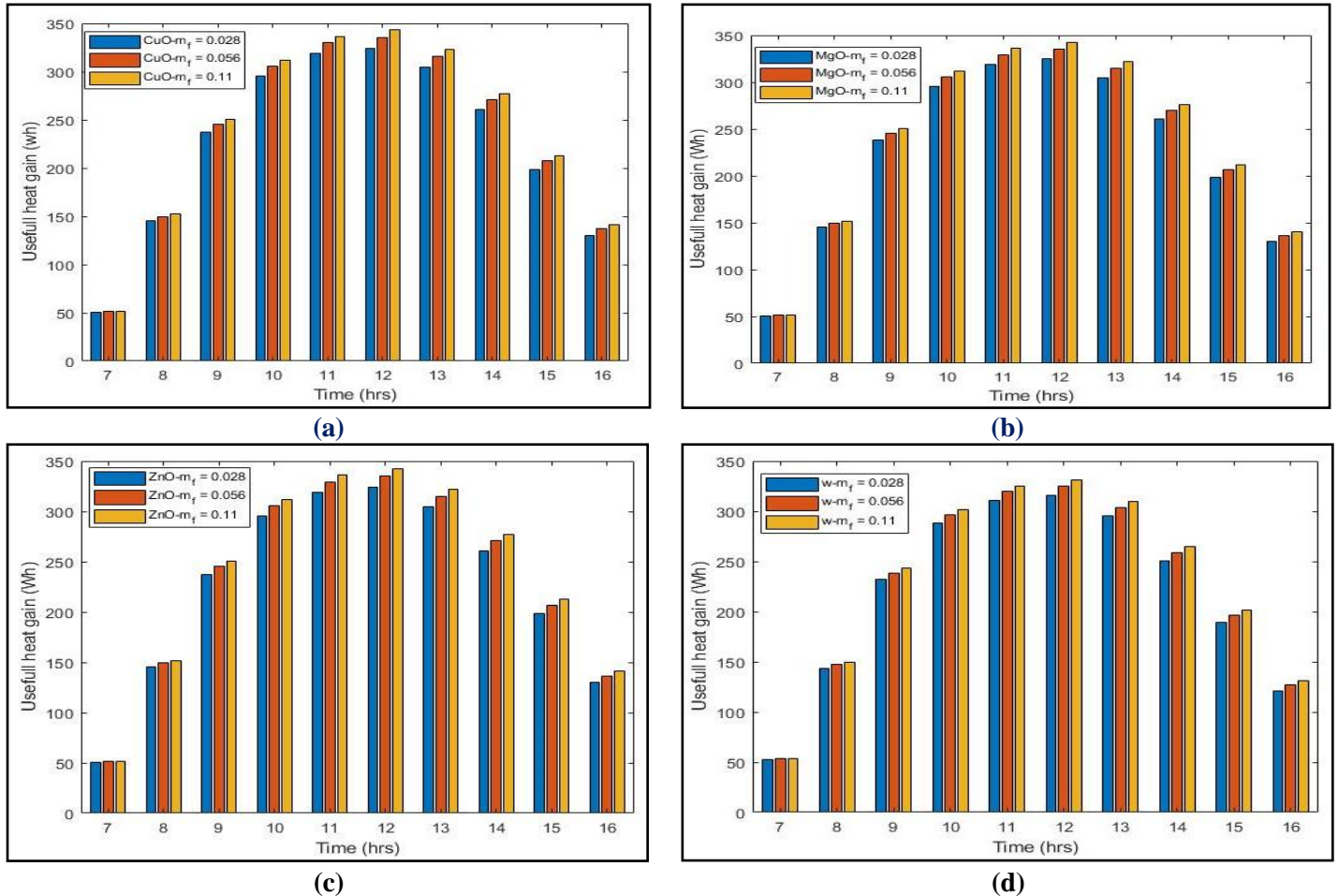


**Figure 10. Hourly fluctuation of heat gain (a) CuO/w (b) MgO/w (c) ZnO/w nanofluid (d) water of PVT system for absorber size 0.03 m.**

Figure 9(a-d) shows the hourly heat gain of the PVT collector using CuO/w, MgO/w, ZnO/ nanofluid, and pure water with size 0.02 m fluid flow channel; heat gain is increased in the morning to 12:00 a.m. and started decreasing from 12:00 a.m. to 04:00 p.m. and maximum heat gain is achieved at 12:00 a.m. it is observed that heat gain increases with increasing the mass flow rate (Al-Shamani et al., 2016). Maximum heat gain is achieved at 345.20 Wh, 344.94 Wh, 344.82, and 333.59 Wh for ZnO/w, CuO/w, MgO/w, and pure water, respectively, at a mass flow rate of 0.11 kg/s.

On the other hand, the fluid flow channel's size is increased by 0.03 m, the hydraulic diameter of the flow channel increases, and valuable heat gain is reduced, as

shown in Figure 10(a-d), because the heat transfer rate is decreased. Hydraulic diameter is inversely proportional to the convective heat transfer coefficient (Hissouf et al., 2020a). In that case, maximum heat gain achieved 345.20 Wh, 344.94 Wh, 344.82 Wh, and 333.59 Wh, respectively, for ZnO/w, CuO/w, MgO/w, and pure water at the same condition. These results show that nanofluids are more effective than water for heat gain because of the high thermal conductivity rate and low specific heat, these two opposing behaviours influence thermal power's

tendency (Jia et al., 2020). Also observed is that lower hydraulics is more effective for the heat gain of the system. Maximum heat gain is achieved in ZnO/w nanofluid compared to the other nanofluids and pure water.

## Thermal efficiency of PVT system

The PVT collector's thermal efficiency is the direct gain of heat generated by the sun energy strike on the absorber sheet over the collector's non-packing area (Han et al., 2021). It is the function of sun radiation, collected heat and the cross-section area of the collector (Lee et al., 2019). In this study, hourly fluctuation of thermal efficiency is evaluated for different nanofluids at 4% volume portion of nanoparticle and pure water for a



triangular shape fluid flow channel with a variation of size 0.02 m and 0.03 m for flow velocity between 0.0005 m/sec to 0.0007 m/s and mass flow rate between 0.028 kg/s to 0.11 kg/s

### Electrical efficiency of PVT system

Electrical efficiency is a direct conversion of sun radiation to electrical current with the help of a PV panel. It is calculated for PV and PVT collectors of different

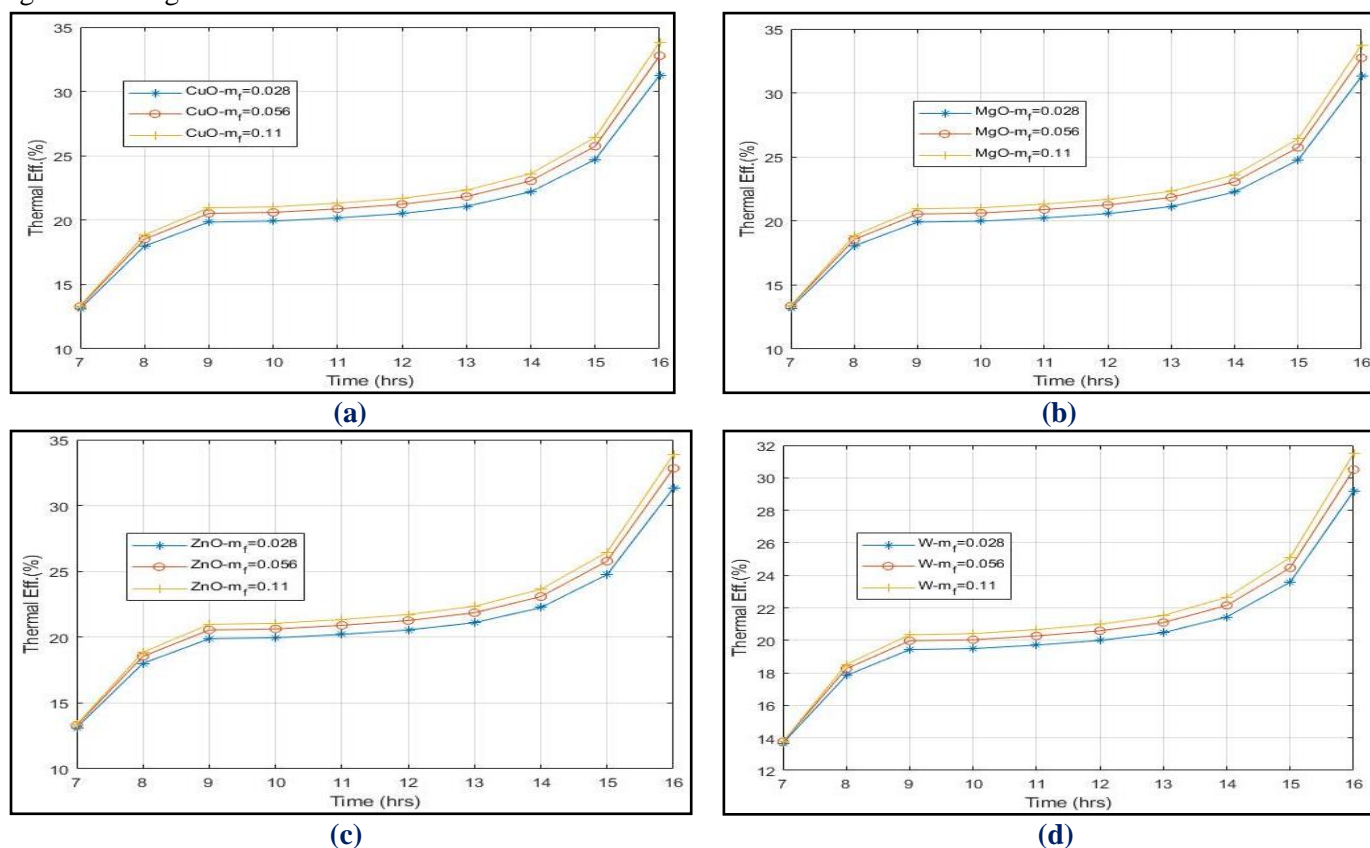
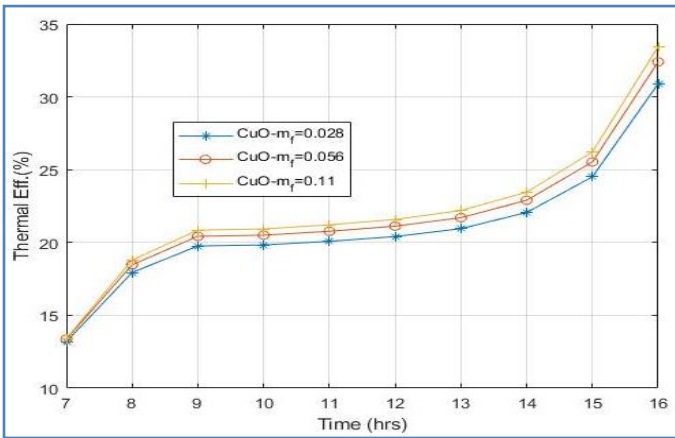


**Figure 11. Hourly fluctuation of thermal efficiency (a) CuO/w (b) MgO/w (c) ZnO/w nanofluid (d) water of PVT system for absorber size 0.02 m.**

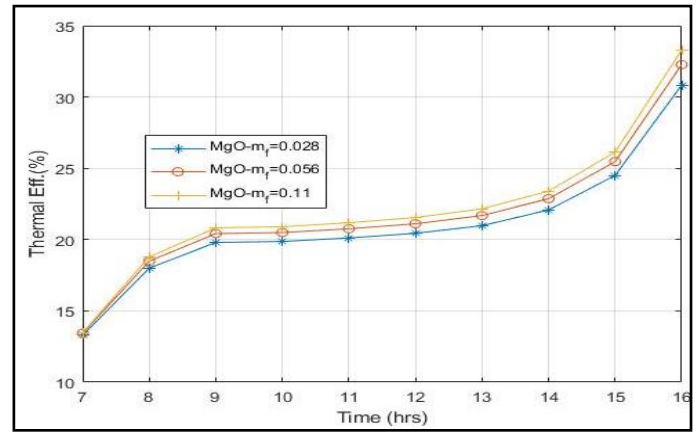
Figure 11(a-d) shows the hourly fluctuation of thermal efficiency of different nanofluids and pure water of 0.02 m size fluid flow channel. It is observed that the mass flow rate is proportional to the thermal performance; by increasing the mass flow rate, the thermal performance also increases (Khanjari et al., 2016). The average thermal efficiency per day achieved for different nanofluids ZnO/w, CuO/w, MgO/w, and pure water is 22.36%, 22.34%, 22.32%, and 21.54%, respectively, at mass flow rates 0.11 kg/s. On the other hand, the size of the fluid flow channel increased by 0.03 m, and the thermal efficiency decreased because the heat transfer rate decreased, as shown in Figure 12(a-d). In this case, the Average thermal efficiency per day achieved for different nanofluids ZnO/w, CuO/w, MgO/w, and pure water is 22.27%, 22.19%, 22.17%, and 21.14%, respectively, at the same mass flow rate. It was observed that higher thermal efficiency is achieved in lower hydraulic diameter and nanofluids compared to higher hydraulic diameter and pure water. Maximum thermal efficiency achieved for ZnO/w nanofluid and 0.02 m fluid flow channel size.

nanofluids at a volume portion of the nanoparticle of 4% and pure water for triangular-shaped fluid flow channels with flow velocity variations between 0.0005 m/s to 0.0007 m/s and the mass flow rate is 0.028 kg/s to 0.112 kg/s with a variation of the size of the flow channel is 0.02 and 0.03 m.

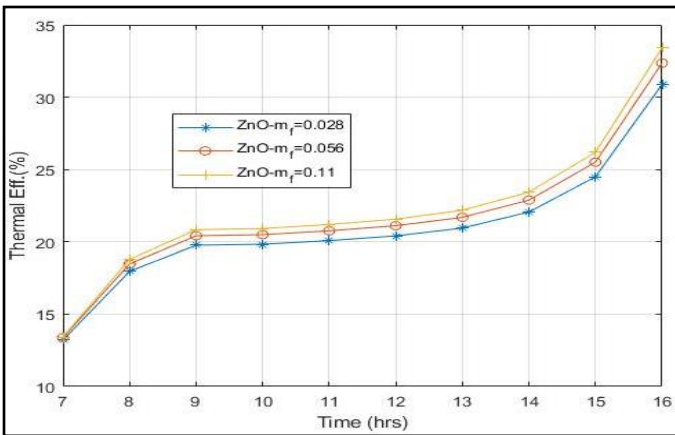
Figure 13(a-d) shows the hourly fluctuation of electrical efficiency with a size 0.02 m isosceles triangular fluid flow channel. Electrical efficiency decreases from morning to 12:00 a.m. and then increases 04:00 p.m. It is observed that electrical efficiency is directly proportional to the mass flow rate and inversely to the cell temperature due to the increased quantity of the mass flow rate, reducing the cell temperature and enhancing the electrical performance (Chow, 2003). Average electrical efficiency per day is achieved for PVT Collector for different nanofluids ZnO/w, CuO/w, MgO/w, and pure water is 14.05%, 14.05%, 14.04% and 13.79%, respectively, at mass flow rate 0.11 kg/s and electrical efficiency of PV is 11.26% the difference between electrical efficiency of PV and PVT is approximately 2.5%. It is clearly shown that the cooling effect improved the electrical performance of the PV panel.



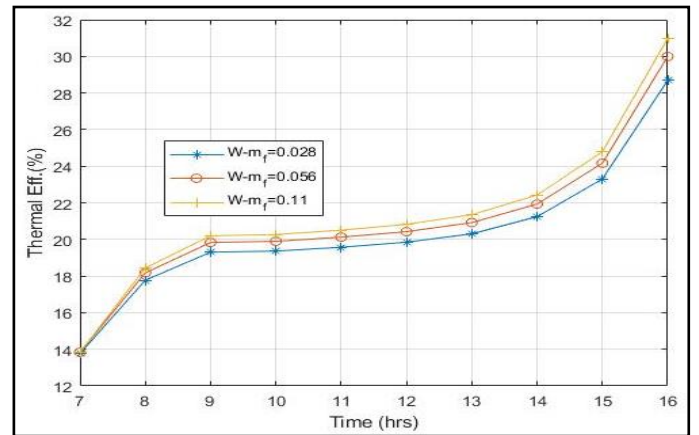
(a)



(b)

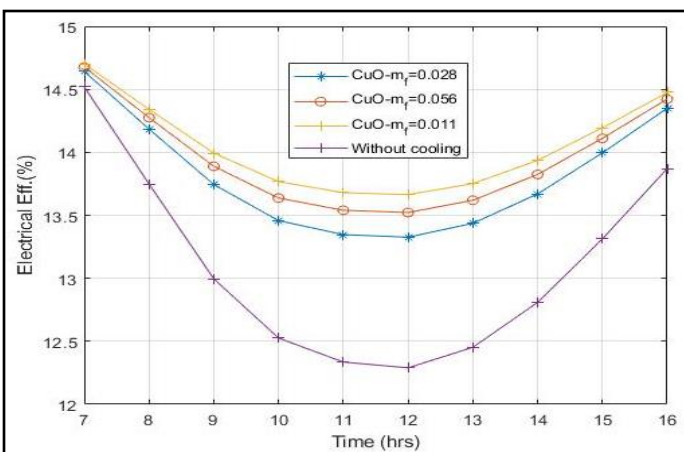


(c)

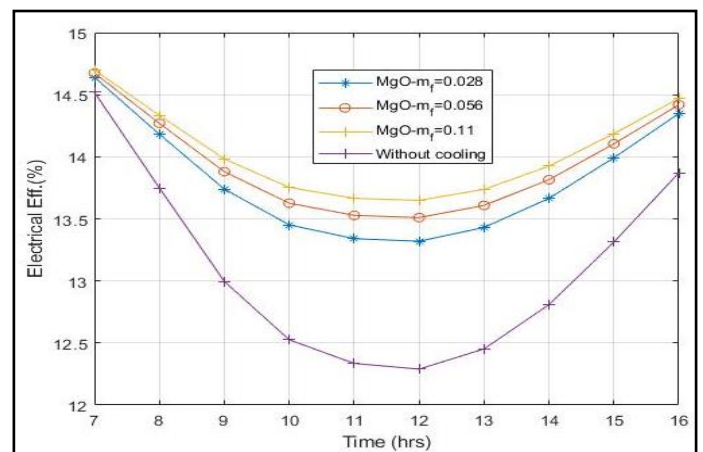


(d)

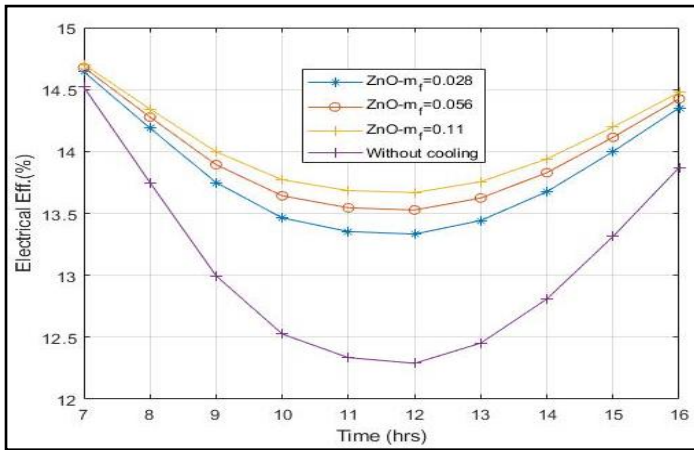
**Figure 12. Hourly fluctuation of thermal efficiency (a) CuO/w (b) MgO/w (c) ZnO/w nanofluid (d) water of PVT system for absorber size 0.03 m.**



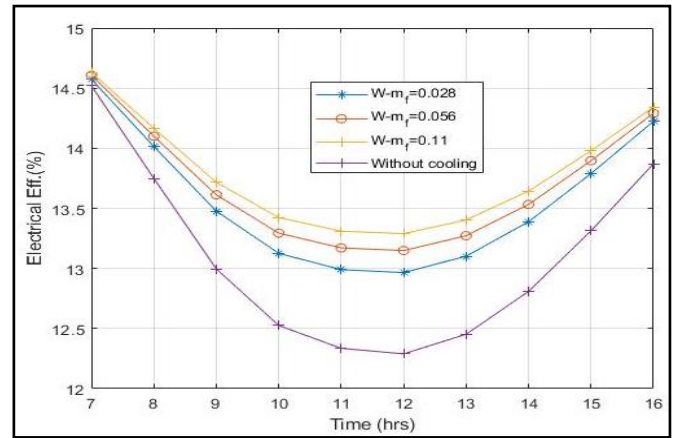
(a)



(b)

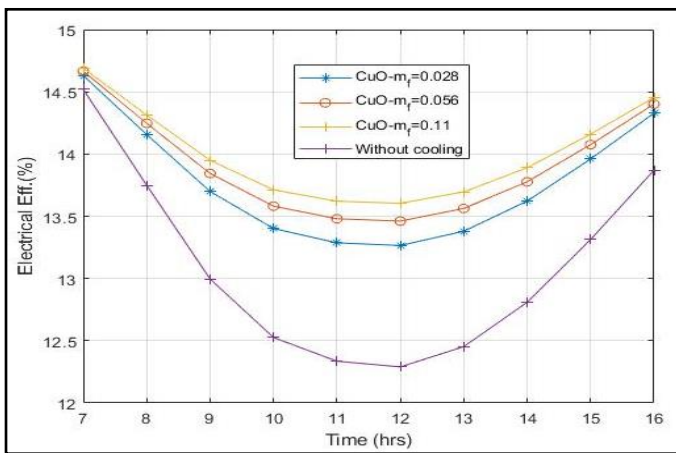


(c)

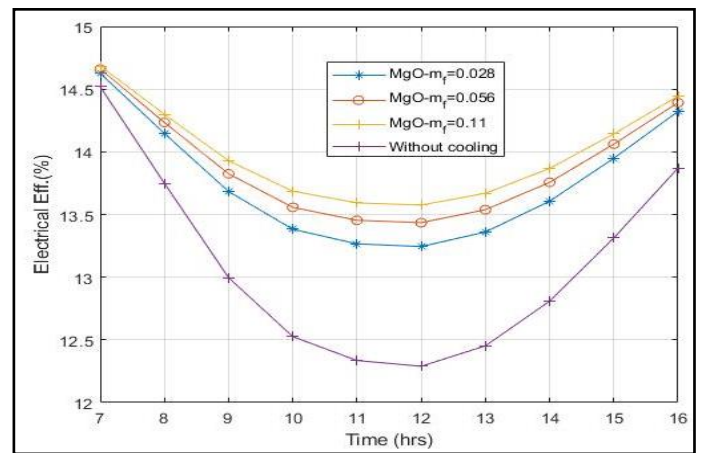


(d)

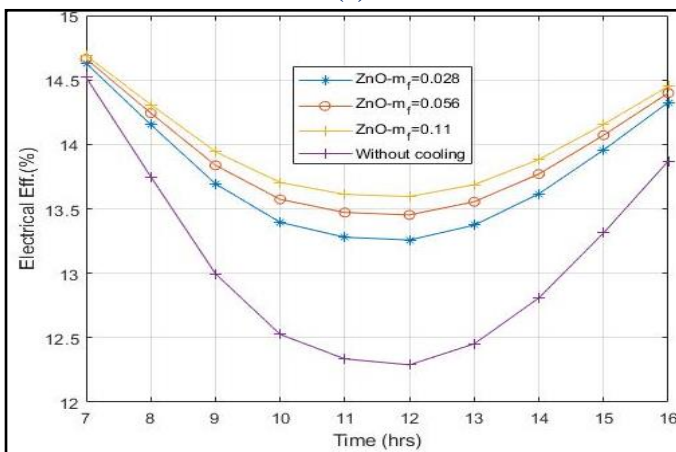
Figure 13. Hourly fluctuation of electrical efficiency (a) CuO/w (b) MgO/w (c) ZnO/w nanofluid (d) water of PVT system for absorber size 0.02 m.



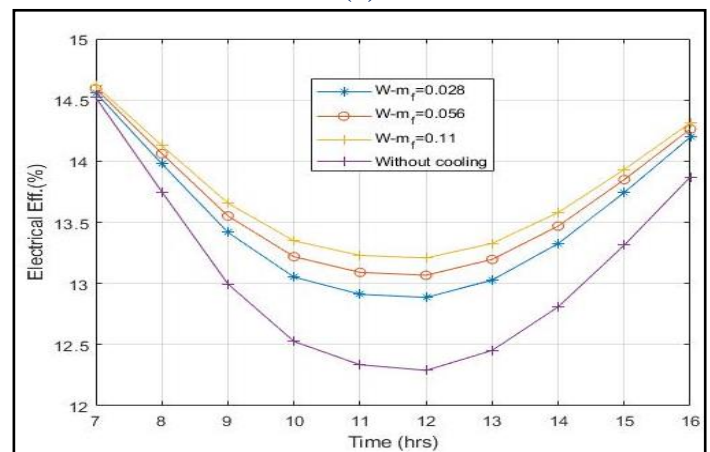
(a)



(b)



(c)



(d)

Figure 14. Hourly fluctuation of electrical efficiency (a) CuO/w (b) MgO/w (c) ZnO/w nanofluid (d) water of PVT system for absorber size 0.03 m.

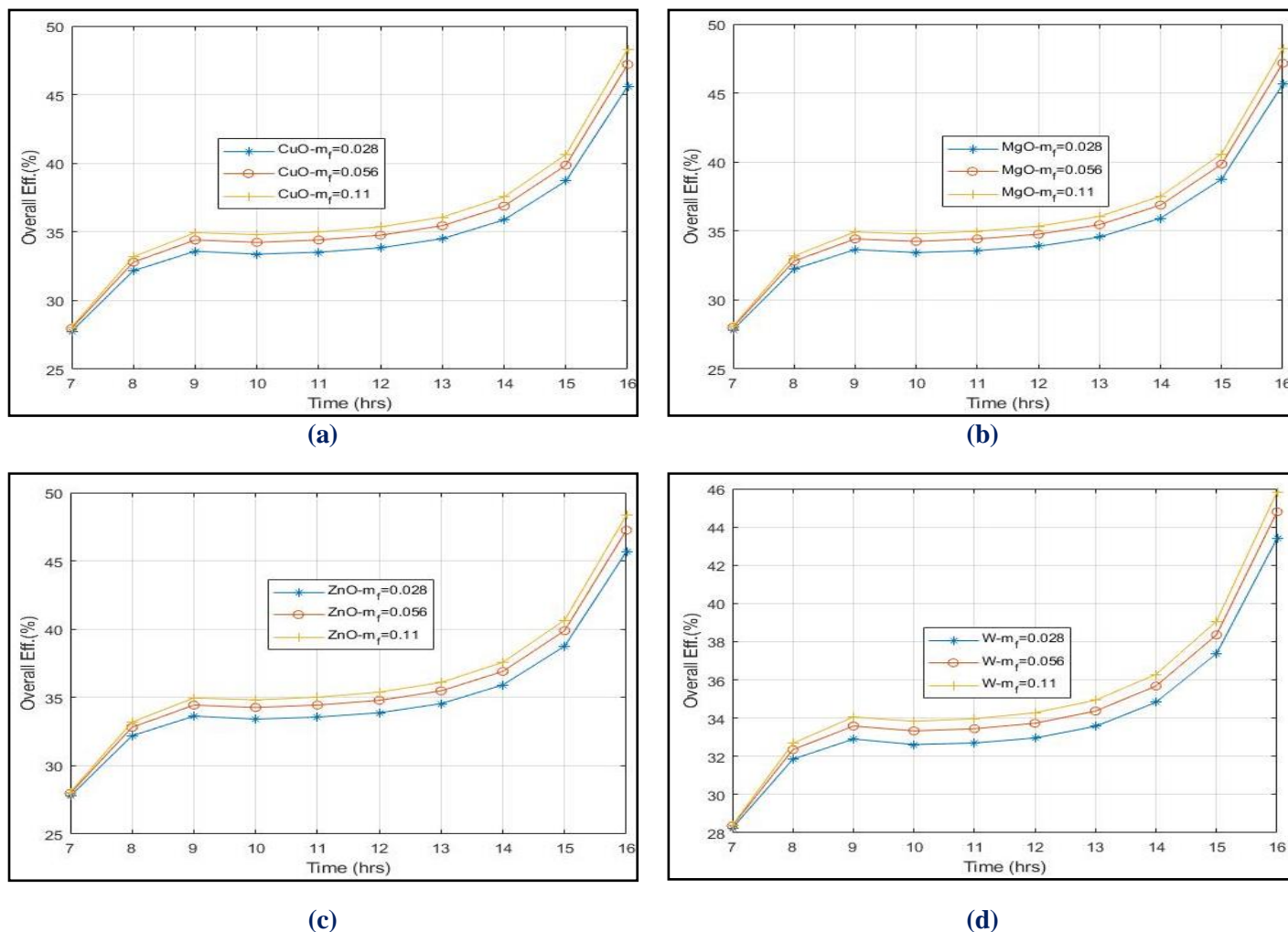


**Figure 15. Hourly fluctuation of overall efficiency (a) CuO/w (b) MgO/w (c) ZnO/w nanofluid (d) water of PVT system for absorber size 0.02 m.**

On the other hand, the size of the fluid flow channel is increased by 0.03 m. Electrical efficiency is reduced because the convective heat transfer coefficient decreases and cell temperature increases, is displayed in Figure 14(a-d). In this case, the Average electrical efficiency per day achieved for PVT Collector for different nanofluids ZnO/w, CuO/w, MgO/w and pure water is 14.02%, 14.00%, 13.98% and 13.73%, respectively, at mass flow rate 0.11 kg/sec. This compression showed that a minor hydraulic diameter is more effective for a better cooling effect, and nanofluids are more effective than water for a high cooling effect. Maximum electrical efficiency is achieved in ZnO/w nanofluid compared to the other coolants.

#### Overall efficiency of PVT system

Overall efficiency is the summation of electrical and thermal efficiency. Figure 15(a-d) shows the hourly fluctuation of the overall efficiency for isosceles

triangular tube size of 0.02 m for different nanofluids ZnO/w, CuO/w, MgO/w at volume portion of nanoparticle is 4% and pure water with the variation of mass flow rate between 0.028 to 0.11 kg/s average overall efficiency of per day is achieved 36.41%, 36.39%, 36.37% and 35.33% respectively.

On the other hand, the size of the fluid flow channel is increased to 0.03 m, and the overall efficiency is decreased. Figure 16(a-d) shows the hourly fluctuation of the overall efficiency for isosceles triangular tube size of 0.03 m for different nanofluids ZnO/w, CuO/w, MgO/w at volume portion 4% and pure water with a variation of mass flow rate between 0.028 to 0.11 Kg/s average overall efficiency of per day is achieved 36.041%, 36.06%, 36.004% and 34.92% respectively at mass flow rate 0.11 kg/sec. Maximum overall efficiency is achieved in ZnO/w nanofluid as compared to the others.



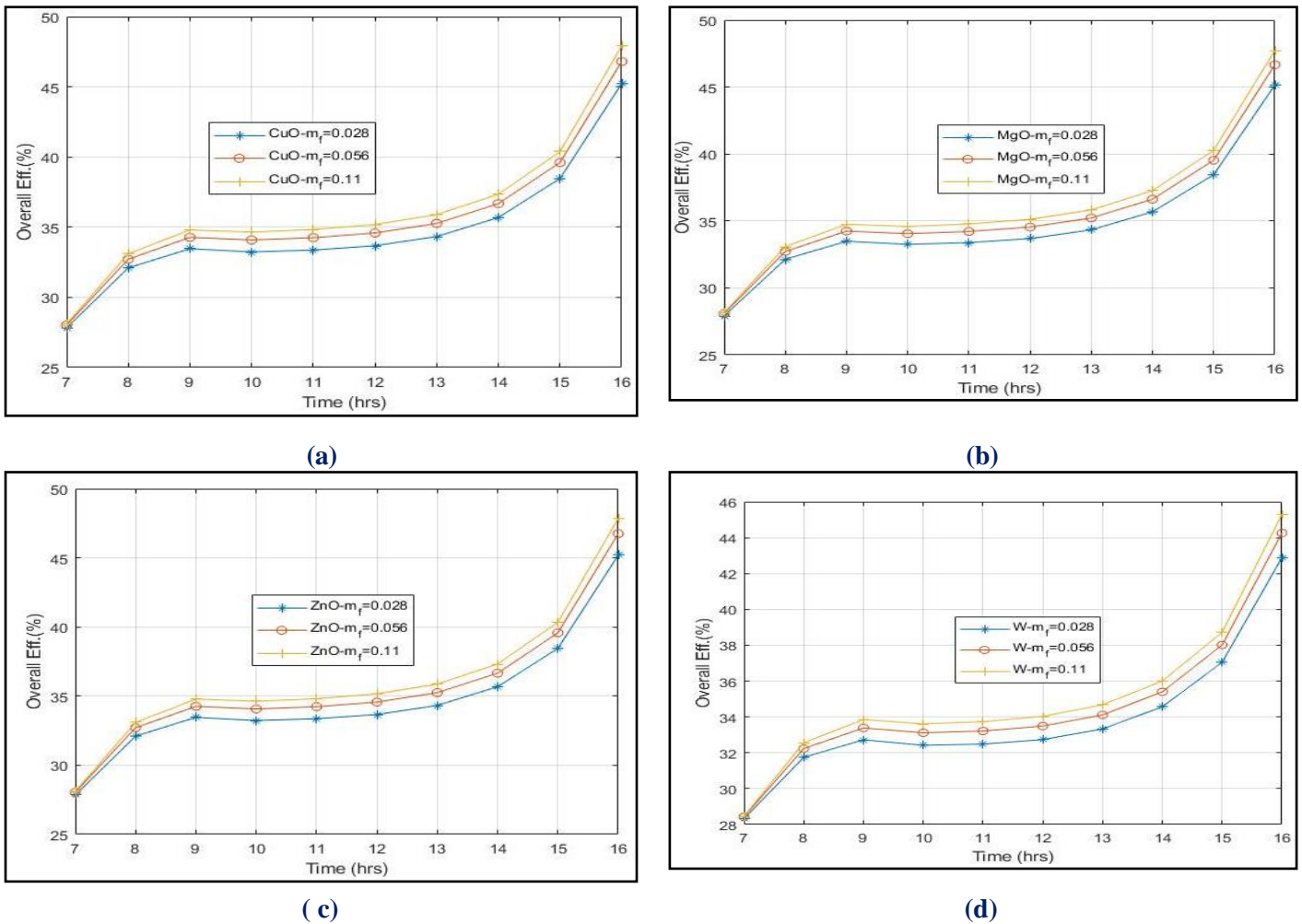


Figure 16. Hourly fluctuation of the overall efficiency (a) CuO/w (b) MgO/w (c) ZnO/w nanofluid (d) water of PVT system for absorber size 0.03 m.

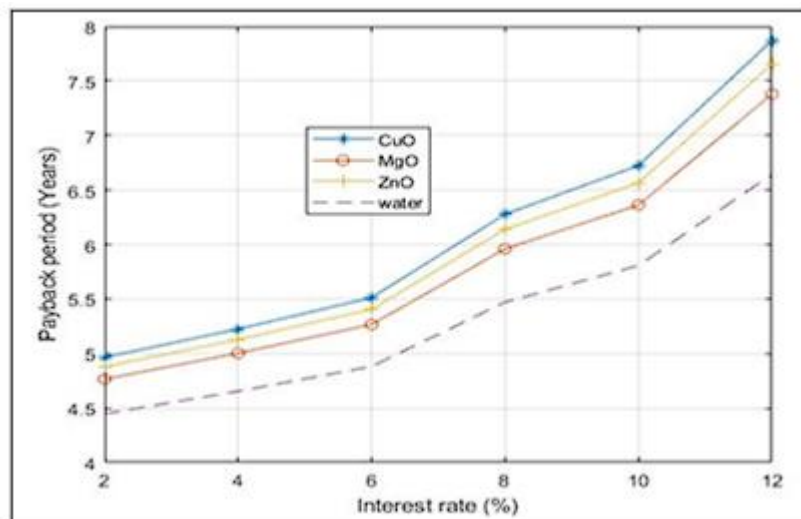


Figure 17. Energy payback duration of PVT collector.

**Economical analysis**

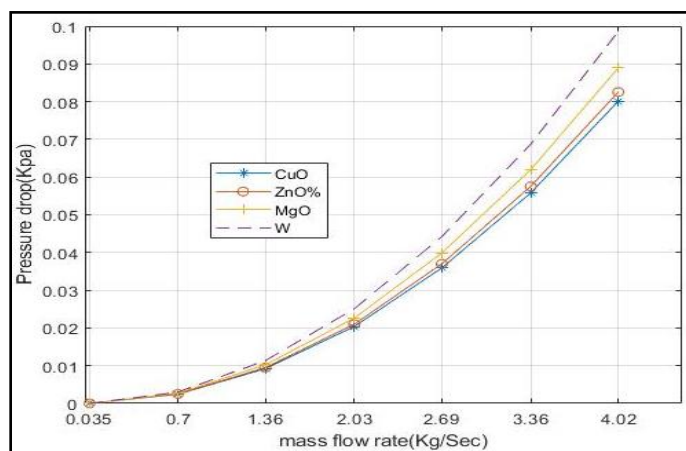
The average sun radiation in India is 5.5 kWh/m<sup>2</sup>/day, and the number of sunshine days is 300 days per year (Jidhesh et al., 2021). The cost of the 250 W

monocrystalline photovoltaic panels is INR. 10000 (\$12.03), and the electricity cost for domestic users in India is 6 INR/kWhr (\$ 0.072). The breakdown cost of the PVT collector is displayed in Figure 3, and The PVT

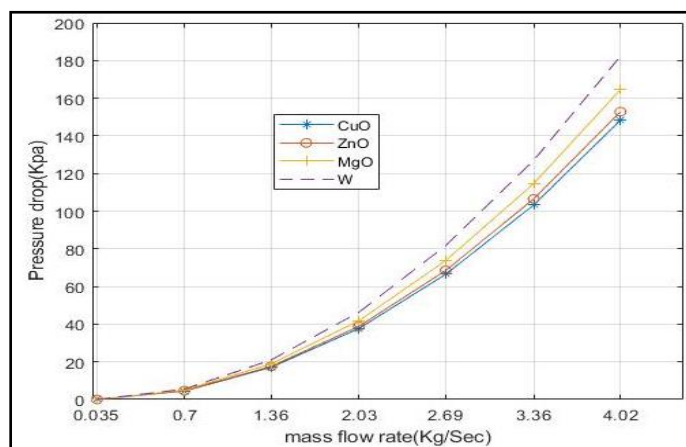
collector's maintenance costs are 10% of the total expense of the system. The payback duration of the PVT collector is calculated for different interest rates displayed in Figure 17. It is observed that the payback duration is directly proportional to the interest rate. The payback duration of PVT collectors using different nanofluid and pure water at a 6% interest rate is 5.5 years, 5.2 years, 5.4 years and 4.8 years for CuO/w, MgO/w, ZnO/w and Pure water, respectively.

### pressure drop

Figure 18(a-b) shows the variation of pressure drop with mass flow rate for different nanofluids and pure water for triangular shape fluid flow channel sizes 0.02 m and 0.03 m. It is observed that an increase in the mass flow rate increases the pressure drop because the pressure drop is a function of velocity (Hissouf et al., 2020b).



(a)



(b)

**Figure 18. Variation of pressure drop (a) channel size 0.02 m (b) channel size 0.03 m.**

Pressure drop achieved for different nanofluids CuO/w, ZnO/w, MgO/w, and pure water is 0.080 kPa, 0.082 kPa, 0.088 kPa and 0.098 kPa, respectively at mass flow rate 4.02 Kg/sec. On the other hand, the size of the

fluid flow channel is increased to 0.03 m. The pressure drop also increases, as shown in Figure 18(b). Pressure drop achieved for different nanofluids CuO/w, ZnO/w, MgO/w, and pure water is 148.2 kPa, 152 kPa, 164 kPa and 182.2 kPa respectively, at mass flow rates 4.02 Kg/s it, is observed that the maximum pressure drop is achieved in water as compared to the nanofluids.

### Conclusions

The present investigation assesses the performance of nanofluid-based PVT collectors utilizing various nanofluids CuO/w, ZnO/w, and MgO/water at a volume portion of the nanoparticle is 4%, alongside pure water as coolants within triangular-shaped fluid flow channels with variations in size 0.02 and 0.03 m and mass flow rates 0.028, 0.056, and 0.11 kg/s. The findings indicate that electrical, thermal, overall efficiency and heat gain are directly proportional to the mass flow rate and inversely proportional to the absorber channel size. Performance parameters decrease with an increase in flow channel size. The maximum average electrical, thermal, overall efficiency and heat gain per day are achieved in ZnO/w nanofluid, reaching 14.57%, 22.36%, 36.41%, and 345.32 Wh, respectively, at a flow velocity of 0.0007 m/s, a mass flow rate of 0.11 kg/s, and a fluid flow channel size of 0.02 m, compared to other nanofluids and pure water. The payback duration of nanofluids-based PVT collectors is 5.5 years, 5.2 years, 5.4 years, and 4.8 years for CuO/w, MgO/w, ZnO/w, and Pure water at a 6% interest rate, respectively. From an economic perspective, the PVT water collector is more efficient, while nanofluids outperform water from an energy perspective. However, pressure losses increase with an increase in fluid flow channel size and mass flow rate. The maximum pressure drop is achieved in water 182.2 Pa for a channel size of 0.03 m compared to nanofluids. As a future aspect, fabricate the experimental setup and validate the numerical results.

### Conflict of Interest

There is no conflict of interest between the authors.

### Acknowledgments

This research work was supported by financial assistance under the fellowship program entitled "Chief Minister Scholarship for Ph.D. on Climate Change" with reference no.: 315253/SKMCCC/EPCO/2021 from the Environmental Planning & Coordination Organization (EPCO), Ministry of Environment, Govt. of Madhya Pradesh, India.

## Nomenclatures

A, c	Area (m <sup>2</sup> ), Specific heat of material (J/kgK )	$U_{tc-a}$	Total heat transfer coefficient from the PV panel to the atmosphere
$d_h$ ,	Hydraulic diameter of the channel (m),	$U_{Lgt}$	Total heat transfer coefficient from bottom to atmosphere
$\dot{F}$	Collector efficiency coefficient	<b>Subscripts</b>	
G	Sun radiation (W/m <sup>2</sup> ),	a, b <sub>s</sub> , b <sub>f</sub> ,	Air, Back surface, Base Fluid
$h_{p1}&h_{p2}$	penalty factor	c, i, o	Solar cell, Inlet, outlet
h	Heat transfer coefficient (W/m <sup>2</sup> K)	g, ref, w	glass, reference, water
k	Rate of heat transfer (W/mK)	eff.	Product of absorptivity and Transmissivity
L, w	Thickness (m), Width (m)	ele, th, n <sub>f</sub> , p,	Electrical, Thermal, Nano Fluid, particle,
$\dot{m}$ & m	Mass flow rate (kg/s.) & Mass (kg),	<b>Greek letters</b>	
$Q_u, T$	Use full heat gain (Wh), Temperature (°C)	$\alpha, \beta, \tau$	Absorptivity, Packing factor, Transmissivity
$U_{tT}$	Heat transmission coefficient from glass to the telder through PV panel	$\eta, \emptyset, \epsilon$	Efficiency, Volume portion, Emissivity
$U_T$	Heat transmission coefficient from the PV panel to the rear surface by conduction	$\rho, \sigma, \mu,$	Density (kg), Stefan Boltzmann constant(W/m <sup>2</sup> k <sup>4</sup> ), Dynamic viscosity (m <sup>2</sup> /s),

## Appendix

Heat transfer between solar cells to atmosphere, solar cell to absorber and fluid to ambient

$$U_{tc-a} = \left[ \frac{L_g}{K_g} + \frac{1}{h_o} \right]^{-1} \quad U_T = \left[ \frac{L_T}{K_T} \right]^{-1} \quad U_{bfa} = \left[ \frac{L_{ins}}{K_{ins}} + \frac{1}{h_i} \right]$$

Convective heat transfer through atmospheric air velocity and total loss coefficient is.

$$h_o = 5.7 + 3.8V \quad h_{cong.g-k} = 2.8 + 3.8V \quad U_{Lgt}$$

$$= U_{tf} + U_{bfa} \quad U_{tf} = \frac{U_{tT} h_{Tf}}{U_{tT} + h_{Tf}}$$

Collector efficiency factor  $\dot{F}$  (Duffie and Beckman, 1991):

$$\dot{F} = \frac{U_L^{-1}}{D \left[ U_L \{d - (D - d)F\}^{-1} + \frac{\delta_b}{K_b} + \pi d_i h_{fi}^{-1} \right]} F$$

$$= \frac{\tanh \left[ m \left( D - \frac{d}{2} \right) \right]}{\left( D - \frac{d}{2} \right)^m}$$

$$= \sqrt{\frac{U_L}{K_{ab} t_{ab}}}$$

Product of absorptivity and Transmissivity  $\alpha \tau_{eff} = \tau_g [\alpha_c \beta_c + \alpha_T (1 - \beta_c) - \alpha_c \eta \beta_c]$

## References

- Agrawal, S., & Tiwari, G. (2015). Performance analysis in terms of carbon credit earned on annualized uniform cost of glazed hybrid photovoltaic thermal air collector. *Solar Energy*, 115, 329-340. <https://doi.org/10.1016/j.solener.2015.02.030>
- Al-Shamani, A. N., Sopian, K., Mat, S., Hasan, H. A., Abed, A. M., & Ruslan, M. (2016). Experimental studies of rectangular tube absorber photovoltaic thermal collector with various types of nanofluids under the tropical climate conditions. *Energy Conversion and Management*, 124, 528-542. <https://doi.org/10.1016/j.enconman.2016.07.052>
- Al-Waeli, A. H., Sopian, K., Kazem, H. A., Yousif, J. H., Chaichan, M. T., Ibrahim, A., Mat, S., & Ruslan, M. H. (2018). Comparison of prediction methods of PV/T nanofluid and nano-PCM system using a measured dataset and artificial neural network. *Solar Energy*, 162, 378-396. <https://doi.org/10.1016/j.solener.2018.01.026>
- Azad, A., Parvin, S., & Hossain, T. (2024). Performance evaluation of nanofluid-based photovoltaic thermal (PVT) system with regression analysis. *Heliyon*, 10(7), e29252. <https://doi.org/10.1016%2Fj.heliyon.2024.e29252>
- Bin Ishak, M. A. A., Ibrahim, A., Sopian, K., Fauzan, M. F., Rahmat, A. A., & Bt Yusaidi, N. J. (2023).

- Performance and economic analysis of a reversed circular flow jet impingement bifacial PVT solar collector. *International Journal of Renewable Energy Development*, 12(4), 780–788.  
<https://doi.org/10.14710/ijred.2023.54348>
- Brinkman, H. C. (1952). The viscosity of concentrated suspensions and solutions. *The Journal of chemical physics*, 20(4), 571-571.  
<https://doi.org/10.1063/1.1700493>
- Buonomano, A., Calise, F., Palombo, A., & Vicidomini, M. (2019). Transient analysis, exergy and thermo-economic modelling of façade integrated photovoltaic/thermal solar collectors. *Renewable Energy*, 137, 109-126.  
<https://doi.org/10.1016/j.renene.2017.11.060>
- Cdivine. *Specification of PV panel*. Retrieved 12-10-2023 from <https://cdivine.com/product/250-watts-mono-crystalline-panel/>
- Charalambous, P., Maidment, G. G., Kalogirou, S. A., & Yiakoumetti, K. (2007). Photovoltaic thermal (PV/T) collectors: A review. *Applied Thermal Engineering*, 27(2-3), 275-286.  
<https://doi.org/10.1016/j.applthermaleng.2006.06.007>
- Chow, T. (2003). Performance analysis of photovoltaic-thermal collector by explicit dynamic model. *Solar Energy*, 75(2), 143-152.  
<https://doi.org/10.1016/j.solener.2003.07.001>
- Deo, N. S., Chander, S., & Saini, J. (2016). Performance analysis of solar air heater duct roughened with multigap V-down ribs combined with staggered ribs. *Renewable Energy*, 91, 484-500.  
<https://doi.org/10.1016/j.renene.2016.01.067>
- Deshmukh, K., & Karmare, S. (2021). A review on convective heat augmentation techniques in solar thermal collector using nanofluid. *J Therm Eng* 7 (5), 1257–1266. In. 10.18186/thermal.978064
- Diwania, S., Siddiqui, A. S., Agrawal, S., & Kumar, R. (2021). Modeling and assessment of the thermo-electrical performance of a photovoltaic-thermal (PVT) system using different nanofluids. *Journal of the Brazilian Society of Mechanical Sciences and Engineering*, 43, 1-18.  
<https://doi.org/10.1007/s40430-021-02909-6>
- Gao, M., Zhu, L., Peh, C. K., & Ho, G. W. (2019). Solar absorber material and system designs for photothermal water vaporization towards clean water and energy production. *Energy & Environmental Science*, 12(3), 841-864.  
<https://doi.org/10.1039/C8EE01146J>
- Gelis, K., Ozbek, K., Ozyurt, O., & Celik, A. N. (2023). Multi-objective optimization of a photovoltaic thermal system with different water based nanofluids using Taguchi approach. *Applied Thermal Engineering*, 219, 119609.  
<https://doi.org/10.1016/j.applthermaleng.2022.119609>
- Gundala, S., Basha, M. M., Madhurima, V., Praveena, N., & Kumar, S. V. (2021). An experimental performance on solar photovoltaic thermal collector with nanofluids for sustainable development. *Journal of Nanomaterials*, 2021, 1-6.  
<https://doi.org/10.1155/2021/6946540>
- Gunnasegaran, P., Mohammed, H., Shuaib, N., & Saidur, R. (2010). The effect of geometrical parameters on heat transfer characteristics of microchannels heat sink with different shapes. *International Communications in Heat and Mass Transfer*, 37(8), 1078-1086.  
<https://doi.org/10.1016/j.icheatmasstransfer.2010.06.014>
- Gupta, A., Agrawal, S., & Pal, Y. (2022). Energy and exergy performance evaluation of a novel photovoltaic-thermoelectric system combined with tube and sheet serpentine water collector. *International Journal of Green Energy*, 19(4), 365-379.  
<https://doi.org/10.1080/15435075.2021.1946814>
- Hamilton, R. L., & Crosser, O. (1962). Thermal conductivity of heterogeneous two-component systems. *Industrial & Engineering chemistry fundamentals*, 1(3), 187-191.  
<https://doi.org/10.1021/i160003a005>
- Han, Z., Liu, K., Li, G., Zhao, X., & Shittu, S. (2021). Electrical and thermal performance comparison between PVT-ST and PV-ST systems. *Energy*, 237, 121589.  
<https://doi.org/10.1016/j.energy.2021.121589>
- Hegedus, S. S., & Luque, A. (2003). Status, trends, challenges and the bright future of solar electricity from photovoltaics. *Handbook of photovoltaic science and engineering*, 1-43.  
<http://dx.doi.org/10.1002/0470014008.ch1>
- Herrando, M., Markides, C. N., & Hellgardt, K. (2014). A UK-based assessment of hybrid PV and solar-thermal systems for domestic heating and power: System performance. *Applied Energy*, 122, 288-309.  
<https://doi.org/10.1016/j.apenergy.2014.01.061>
- Hissouf, M., Najim, M., & Charef, A. (2020a). Numerical study of a covered Photovoltaic-Thermal Collector



- (PVT) enhancement using nanofluids. *Solar Energy*, 199, 115-127.  
<https://doi.org/10.1016/j.solener.2020.01.083>
- Hissouf, M., Najim, M., & Charef, A. (2020b). Performance of a photovoltaic-thermal solar collector using two types of working fluids at different fluid channels geometry. *Renewable Energy*, 162, 1723-1734. 1734.  
<https://doi.org/10.1016/j.renene.2020.09.097>
- Hussain, M. I., & Kim, J.-T. (2018). Conventional fluid- and nanofluid-based photovoltaic thermal (PV/T) systems: A techno-economic and environmental analysis. *International Journal of Green Energy*, 15(11), 596-604.  
<https://doi.org/10.1080/15435075.2018.1525558>
- Javadi, F. S., Saidur, R., & Kamalisarvestani, M. (2013). Investigating performance improvement of solar collectors by using nanofluids. *Renewable and Sustainable Energy Reviews*, 28, 232-245.  
<https://doi.org/10.1016/j.rser.2013.06.053>
- Jia, Y., Ran, F., Zhu, C., & Fang, G. (2020). Numerical analysis of photovoltaic-thermal collector using nanofluid as a coolant. *Solar Energy*, 196, 625-636.  
<https://doi.org/10.1016/j.solener.2019.12.069>
- Jidhesh, P., Arjunan, T., & Gunasekar, N. (2021). Thermal modeling and experimental validation of semitransparent photovoltaic-thermal hybrid collector using CuO nanofluid. *Journal of Cleaner Production*, 316, 128360.  
<https://doi.org/10.1016/j.jclepro.2021.128360>
- Kamthania, D., Nayak, S., & Tiwari, G. (2011). Performance evaluation of a hybrid photovoltaic thermal double pass facade for space heating. *Energy and Buildings*, 43(9), 2274-2281.  
<https://doi.org/10.1016/j.enbuild.2011.05.007>
- Kazem, H. A., Al-Waeli, A. H., Chaichan, M. T., Al-Waeli, K. H., Al-Aasam, A. B., & Sopian, K. (2020). Evaluation and comparison of different flow configurations PVT systems in Oman: A numerical and experimental investigation. *Solar Energy*, 208, 58-88. <https://doi.org/10.1016/j.solener.2020.07.078>
- Khan, A. A., Danish, M., Rubaiee, S., & Yahya, S. M. (2022). Insight into the investigation of Fe<sub>3</sub>O<sub>4</sub>/SiO<sub>2</sub> nanoparticles suspended aqueous nanofluids in hybrid photovoltaic/thermal system. *Cleaner Engineering and Technology*, 11, 100572.  
<https://doi.org/10.1016/j.clet.2022.100572>
- Khanjari, Y., Pourfayaz, F., & Kasaeian, A. (2016). Numerical investigation on using of nanofluid in a water-cooled photovoltaic thermal system. *Energy Conversion and Management*, 122, 263-278.  
<https://doi.org/10.1016/j.enconman.2016.05.083>
- Kong, X., Zhang, Y., Wu, J., & Pan, S. (2022). Numerical Study on the Optimization Design of Photovoltaic/Thermal (PV/T) Collector with Internal Corrugated Channels. *International Journal of Photoenergy*. <https://doi.org/10.1155/2022/8632826>
- Lee, J. H., Hwang, S. G., & Lee, G. H. (2019). Efficiency improvement of a photovoltaic thermal (PVT) system using nanofluids. *Energies*, 12(16), 3063.  
<https://doi.org/10.3390/en12163063>
- Madas, S. R., Narayanan, R., & Gudimetla, P. (2023). Numerical investigation on the optimum performance output of photovoltaic thermal (PVT) systems using nano-copper oxide (CuO) coolant. *Solar Energy*, 255, 222-235.  
<https://doi.org/10.1016/j.solener.2023.02.035>
- Madhesh, D., & Kalaiselvam, S. (2015). Experimental study on heat transfer and rheological characteristics of hybrid nanofluids for cooling applications. *Journal of Experimental Nanoscience*, 10(15), 1194-1213.  
<https://doi.org/10.1080/17458080.2014.989551>
- Mahmood Alsalame, H. A., Lee, J. H., & Lee, G. H. (2021). Performance Evaluation of a Photovoltaic Thermal (PVT) system using nanofluids. *Energies*, 14(2), 301. <https://doi.org/10.3390/en14020301>
- Nasrin, R., Rahim, N. A., Fayaz, H., & Hasanuzzaman, M. (2018). Water/MWCNT nanofluid based cooling system of PVT: Experimental and numerical research. *Renewable Energy*, 121, 286-300.  
<https://doi.org/10.1016/j.renene.2018.01.014>
- Pak, B. C., & Cho, Y. I. (1998). Hydrodynamic and heat transfer study of dispersed fluids with submicron metallic oxide particles. *Experimental Heat Transfer an International Journal*, 11(2), 151-170.  
<https://doi.org/10.1080/08916159808946559>
- Power, M. O. (2023). *Report of power generation* Retrieved 15- 10 -2023 from:  
<https://powermin.gov.in/>
- Rejeb, O., Dhaou, H., & Jemni, A. (2015). Parameters effect analysis of a photovoltaic thermal collector: Case study for climatic conditions of Monastir, Tunisia. *Energy Conversion and Management*, 89, 409-419.  
<https://doi.org/10.1016/j.enconman.2014.10.018>
- Resources, N. E. (2023). *Provides solar and meteorological data sets from NASA research for support of renewable energy, building energy efficiency and agricultural needs*. Retrieved 10-10-

- 2023 from <https://power.larc.nasa.gov/data-access-viewer/>
- Sani, E., Barison, S., Pagura, C., Mercatelli, L., Sansoni, P., Fontani, D., Jafrancesco, D., & Francini, F. (2010). Carbon nanohorns-based nanofluids as direct sunlight absorbers. *Optics Express*, 18(5), 5179-5187. <https://doi.org/10.1364/OE.18.005179>
- Sardarabadi, M., & Passandideh-Fard, M. (2016). Experimental and numerical study of metal-oxides/water nanofluids as coolant in photovoltaic thermal systems (PVT). *Solar energy materials and solar cells*, 157, 533-542. <https://doi.org/10.1016/j.solmat.2016.07.008>
- Sardarabadi, M., Passandideh-Fard, M., & Heris, S. Z. (2014). Experimental investigation of the effects of silica/water nanofluid on PV/T (photovoltaic thermal units). *Energy*, 66, 264-272. <https://doi.org/10.1016/j.energy.2014.01.102>
- Somasundaram, S., & Tay, A. A. (2019). Performance study and economic analysis of photo-voltaic thermal system under real-life thermal loads in tropical climate. *Sustainable Environment Research*, 29, 1-10. <https://doi.org/10.1186/s42834-019-0040-5>
- Tiwari, A., & Sodha, M. (2006). Performance evaluation of hybrid PV/thermal water/air heating system: a parametric study. *Renewable Energy*, 31(15), 2460-2474. <https://doi.org/10.1016/j.renene.2005.12.002>
- Tiwari, A., Sodha, M., Chandra, A., & Joshi, J. (2006). Performance evaluation of photovoltaic thermal solar air collector for composite climate of India. *Solar Energy Materials and Solar Cells*, 90(2), 175-189. <https://doi.org/10.1016/j.solmat.2005.03.002>
- Yu, C., Li, H., Chen, J., Qiu, S., Yao, F., & Liu, X. (2021). Investigation of the thermal performance enhancement of a photovoltaic thermal (PV/T) collector with periodically grooved channels. *Journal of Energy Storage*, 40, 102792. <https://doi.org/10.1016/j.est.2021.102792>
- Zhou, J., Ke, H., & Deng, X. (2018). Experimental and CFD investigation on temperature distribution of a serpentine tube type photovoltaic/thermal collector. *Solar Energy*, 174, 735-742. <https://doi.org/10.1016/j.solener.2018.09.063>

#### How to cite this Article:

Mrigendra Singh, S.C Solanki, Basant Agrawal and Rajesh Bhargava (2024). Performance Evaluation and Cost Analysis of Photovoltaic Thermal (PVT) System Using the Triangular Shape of Absorber with Different Water-based Nanofluids as Coolants. *International Journal of Experimental Research and Review*, 39(spl.) 51-72.

DOI:<https://doi.org/10.52756/ijerr.2024.v39spl.004>



This work is licensed under a Creative Commons Attribution-NonCommercial-NoDerivatives 4.0 International License.